SAFE

Slow Active Faults in Europe

**Assessing fundamental input for seismic risk assessment in regions of low seismicity**

**Project No: EVG1-2000-22005**
**Call Identifier: EESD-ENV-99-2-C**
**Thematic Priorities: 1.1.4.-7.1.**

**Partner 2 – Istituto Nazionale di Geofisica e Vulcanologia (Rome, Italy)**

# WP8 | MODELLING OF TOPOGRAPHIC SIGNAL

# DETAILED CHARACTERISATION OF INDIVIDUAL STRUCTURES

## (Deliv 8.2)

**Editor: G. Valensise**

**Writers: A. Astori, R. Basili, P. Burrato, G. Valensise, P. Vannoli, (INGV, partner #2)**

**Collaborators: E. Baroux (INGV), F. Ciucci (INGV), D. Massoli (University of Perugia and INGV)**

Introduction

This deliverable will describe in detail results obtained during the project for four key areas of the Po Plain, the target area for the INGV contribution to the project. The four area are:

1) Coastal Marche region (southeastern Po Plain – see Section 1)
2) Mantova/Mincio River area (central Po Plain – see Section 2)
3) Mirandola/Secchia-Panaro Rivers area (southern-central Po Plain – see Section 3)
4) Soncino/Oglio River area (western Po Plain – see Section 4)

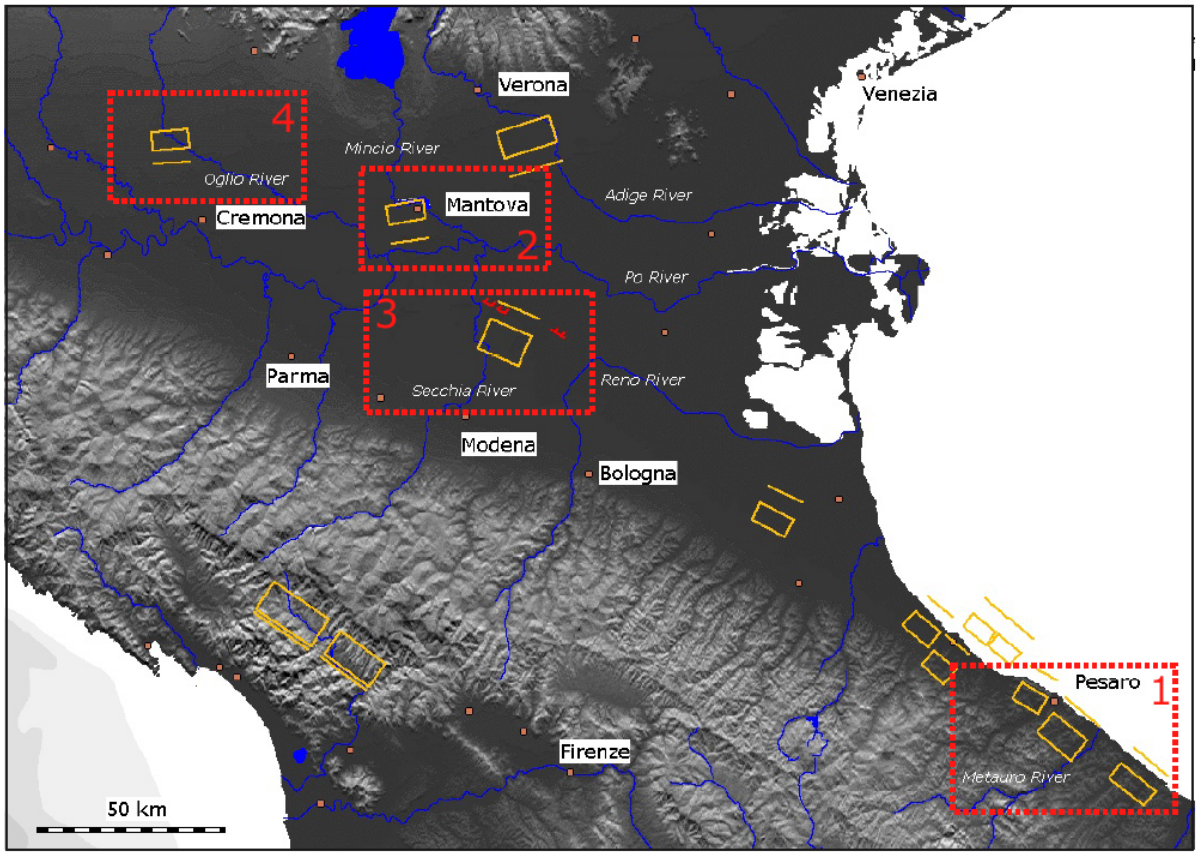

# Section 1 – The coastal Marche region (southeastern Po Plain)

**by Paola Vannoli, Roberto Basili and Gianluca Valensise**

## *1.1. Introduction*

It was not until the late 1980s that blind faulting caught the attention of the seismological community. This awareness certainly dawned in California after the 1983, Coalinga (Mw 6.5: Stein and Ekström, 1992) and 1987, Whittier Narrows (Mw 5.9: Shaw and Shearer, 1999) damaging earthquakes, both associated with blind faults. The 1994 Northridge earthquake (Mw 6.7) also ruptured a blind and previously unmapped fault (Scientists of the U.S.G.S. and S.C.E.C., 1994). Meanwhile in Italy the same interest crept ahead as blind faults were found to have originated both historical and recent earthquakes. For example, a previously unknown, blind, low-angle normal fault was blamed for the highly destructive 1908, Mw 7.0 Messina Straits earthquake (e.g. Valensise and Pantosti, 1992). Similarly, combined geological, seismological and geodetic evidence showed that the three major shocks of the 1997 Umbria-Marche earthquake sequence (Mw 5.6, 5.9, 5.5) occurred on blind normal faults that have little to do with the well-known normal faults exposed in the area (e.g. Barba and Basili, 1999; Amato and Cocco, 2000). New worries are growing concerning many thrust faults buried beneath the Po Plain where seismic risk is all but negligible (Burrato et al., 2003). In the rest of Europe, blind faulting is being invoked to explain the occurrence of significant historical earthquakes such as the 1909, Lambesc (southern France, Mw 6.0: Baroux et al., 2003) and the 1428 Queralbs (northern Spain, Me 6.6: Philip et al., 1992).

It is widely acknowledged that blind faults pose a stealthy threat in seismic prone areas, and their list would grow enormously if examples from the rest of the world were included. Yet, investigations on blind faulting are limited in comparison with the work done on surface-breaking faults. Short faults (~10 km) capable of M~6 earthquakes and characterised by long repeat times (≥1,000 y) receive even less attention, even if they occur in highly populated areas. Nevertheless, a growing community is becoming aware of the need to set aside the investigation of large well-expressed faults and focus on many problematic cases that exist all throughout Europe (for example within the EU project SAFE - Slow Active Faults in Europe: Sebrier et al., 2003).

Small blind faults capable of infrequent moderate-size earthquakes clearly produce only subtle displacement of the ground surface. Therefore, it does not surprise that classical geological investigations fall short in detecting such displacement, even after it accumulated over several seismic cycles. This is why blind faults are rarely hunted and most still unmapped. Can we improve our ability to identify them? Perhaps, if we put to a sensible use a very sensitive tool. Drainage and coastal systems are known to respond very efficiently to even the faintest vertical modification of the ground surface induced by a buried fault. Analysing their associated geomorphic features (channel migrations/avulsions, raised/warped terraces, bedding attitudes) may return basic but robust information on the geometry and kinematics of perfectly invisible faults. This is especially useful in seismic hazard applications because the typical scale of these geomorphic indicators and their fluctuations (~5-10 km) naturally filter out strains associated with tectonic features that are too small or shallow to be seismogenic. A similar approach has been successfully applied to reconstruct the geometry of large compressional blind faults in Southern California (Rockwell et al., 1988; Keller et al., 1998) and to predict the size and slip rate of a blind thrust in the California offshore (Ward and Valensise, 1996). Similar techniques were recently tested also on faults lying beneath the Po Plain, northern Italy (Benedetti et

al., 2000; Burrato et al., 2003), that share a similar tectonic style and climatic environment with the area investigated in this work.

We propose to apply a similar method to the northern Marche coastal belt, central Italy, that is affected by significant historical and instrumental seismicity (**Figure 1**). This area is also characterised by NW-SE trending compressional structures but no mapped fault is exposed, at least not one that could be blamed for one of the earthquakes that occurred in the region. On the basis of the perspective outlined above we searched for clues of the relationships between earthquakes and their possibly blind causative faults. We analysed geomorphic features related with the most recent developments of the drainage network and its correlative coastal system. Our approach aims at detecting any departure from the normal behaviour of a drainage system in a non-tectonic area. The study was conducted at two different wavelengths to discriminate the contributions of regional (100 km) and local (10 km) tectonic processes.

The purpose of this paper is to (1) demonstrate that there is more than a clue that the northern Marche coastal belt is seismically threatened by blind thrust faults; (2) contribute to provide the basic information to identify and characterise these faults; and (3) help estimate their earthquake potential. Although a fault segmentation model of this area has already been proposed on a broad geological basis (Valensise and Pantosti, 2001), so far risk mitigation plans at all scales (national, regional) have little considered the potential contribution of an organised fault system. We believe that our results will bring forward a new understanding of the seismic build-up-and-release process in this area.

## *1.2. Tectonic setting and seismicity*

The northern Marche coastal belt stretches along the foothills on the eastern side of the Apennine range, an accretionary prism whose growth is driven by north-eastward stacking of thrust sheets. The Apennine thrust front has progressively migrated toward the east-northeast all through the Tertiary - Quaternary and is thought to be currently active just a few kilometres off the Adriatic coast (e.g. Elter et al., 1975; Doglioni et al., 1998). Tectonic uplift of the anticlinorium is greater in its interiors and lessens progressively north-eastward (e.g. Lipparini, 1939). Local-scale tectonic movements also affect its forelimb (e.g. Elmi et al., 1987; Nanni and Vivalda, 1987; Nesci et al., 1990). It is also widely agreed that the seismicity of the Adriatic coast is due to the activity of the frontal thrusts (e.g. Lavecchia et al., 1994; Frepoli and Amato, 1997). Basili (2001) and Basili and Valensise (2001) proposed a segmentation model of the Apennine frontal thrust system, blaming individual blind thrust faults for the occurrence of the largest earthquakes of the Adriatic coastal belt and identifying two potential seismic gaps.

Conversely, Coward et al. (1999) stated that thrusting and folding, at the mountain front, ended in the Early Pleistocene. Based on a postulated lack of significant compressional deformation in Middle-Late Pleistocene deposits of the Adriatic offshore, Di Bucci and Mazzoli (2002) supported this view, adding that NE-SW extension and NW-SE compression dominate the area today. Savelli et al. (2002) proposed that active (Late Pleistocene?) WSW-ENE extension is progressively replacing the inactive compression and currently extends as far out as 25 km upstream in the Metauro River valley.

The northern Adriatic coast, however, apparently belongs to the same thrust system buried in the Po Plain that is known to have released a number of compressional earthquakes (Frepoli and Amato, 1997). In addition, borehole breakouts data indicate a minimum horizontal stress axis striking NW-SE on average (Montone et al., 1999). Breakouts and focal mechanisms combined indicate that the orientation of compression at the thrust front is about NE-SW. The focal solution of the 1987, Porto San Giorgio earthquake ($M_w$ 5.1), that occurred 50 km southeast of Ancona, clearly indicates NE-SW horizontal compression (P axis strikes 212° and dips 0°, Montone et al., 1999; solution obtained through the Regional Centroid Moment Tensors algorithm: Arvidsson and Ekström, 1998; Pondrelli et al., 2002). A recent sequence including five events in the magnitude range $M_w$ 4.1 - 4.8 that took place in the Forlì area, 50 km northwest of Rimini, yielded focal mechanisms with nearly horizontal N214-240 striking P-axes (Pondrelli et al., 2002). Historical seismicity also suggests that compressional stress

controls the release of seismic energy in this area. Several earthquakes having equivalent magnitude ($M_e$) larger than 5 (**Table 1**, **Figure 1**) stroke the northern Adriatic coastal area in the past few centuries (Gruppo di Lavoro CPTI, 1999). They line up in the NW-SE direction, roughly parallel to the coast; their intensity distributions are elongated likewise, and some originated a tsunami (Boschi et al., 2000). The occurrence of tsunami indicates that the earthquakes occurred close to the coast or offshore and that their causative faults have been able to produce significant vertical displacement of the sea floor; thus, the ruptures should have had a dominant dip-slip component.

## 1.3. Geomorphic data

### 1.3.1. Generalities

The area under examination is a 70 km-long and 30 km-wide hilly belt, stretching NW-SE along the coast of northern Marche (**Figure 2**). It is bounded to the south-west by the northern Apennines range, where the Conca, Foglia, Metauro, Cesano, Misa, and Esino rivers originate. They all drain north-eastward along a route orthogonal to the trend of the main geological structures. Their valleys are carved into Meso-Cenozoic bedrock evolving upward from carbonate-prevalent to terrigenous. The Miocene harder rocks generally dwindle north-eastward, where they are blanketed by Pliocene-Pleistocene poorly consolidated and easily erodible marine formations. The lowermost reaches of the river valleys, where the river channels seemingly flow undisturbed, extend smoothly through these latter formations. Aggradational processes and resulting sediments dominate here. Nonetheless, drainage anomalies of various sorts, such as lateral channel migration or change from aggradation to degradation in the channel pattern, are easily identified locally and have long been known.

Along the coastal slope and along the major river valley walls we identified coastal and fluvial terraces, respectively. The first three lower and younger orders are often very well preserved, together with their sedimentary bodies, and could be followed almost continuously even at the transition from the fluvial to the coastal domain. Several remnants are seen scattered above and below the main levels. The higher and older (from the fourth upward) orders are much more dissected, remodelled, and often stripped of their deposits.

We reconstructed the various orders based on lateral continuity of the various remnants, the accordance of their elevations at short distance, and the similarity of the vertical spacing between treads. In the lower reaches of the valleys, present-day river channels are mostly entrenched on the south-eastern side. Thus, the north-western wall of the valleys is generally draped by the most complete step-like series of terrace treads, while only smaller remnants are preserved on the opposite side.

In this section, we will first illustrate the main features of the first three younger terrace orders, for they provide the most important clues for the purpose of this paper, and very briefly the higher orders. We will then describe a few local drainage anomalies that were found mainly in the lower reaches of the analysed rivers.

### 1.3.2. Coastal terraces

The first order terrace (*C1*) extends widely only in the northern 50 km of the coastal belt, where its remnants are several kilometres long and up to 1 km-wide. At river outlets the terrace top surface generally exhibits a seamless transition into its fluvial correlative. Locally, terrace remnants end against an outcrop of Miocene-Pliocene bedrock carved by a 200 m high cliff. Its inner edge is well preserved and rather continuous. It also clearly marks the contact between this terrace and the depositional body of the higher, and thus older, terrace. However, at the mouth of the Conca River the ter-

race adjoins an outcrop of Miocene sandstone bedrock and its inner edge marks the bottom of an inactive cliff for about 700 m. The terrace inner edge elevation varies, from North to South, between 8 and 4 m. Due to the relatively low elevation, its outer edge and slope are often adjoined by present-day sandy beaches and its top surface is sometimes covered by littoral dunes. Although the depositional body of the terrace is never exposed (mainly because of the late dense urbanisation), several geomorphic features, such as fossil dunes and long-shore bars, confirm the depositional origin of the terrace.

The second order terrace (*C2*) stretches continuously along the whole coastal belt, except for few places where it ends against Miocene bedrock. It is the widest and the best preserved terrace of the sequence. Its top surface is over 1 km-wide between the mouths of the Metauro and Cesano Rivers and narrows southward. To the north, at the Conca River mouth, its top surface continues seamlessly into an over 6 km-wide remnant of an alluvial plain. The terrace inner edge marks the contact between the depositional body and the underlying bedrock. The elevation of the inner edge is 16 m at the mouth of the Conca River, about 16 m between the Arzilla and Cesano Rivers, and as low as 4 m at the Misa and Esino River mouths. Just south of the Cesano River mouth, the depositional body of the terrace is exposed for a height of about 5 m below its top surface. Few-centimetre-thick layers of yellow laminated and sometimes cross-bedded sands alternate with yellow-grey massive clays. Lens-shaped gravel bodies, up to 0.2 m-thick and 7 m-wide, also intercalate unevenly. Noticeably, the sediment layers generally dip slightly (<2°) south-westward, i.e. counter-slope, suggesting the body may have undergone some gentle tilting after deposition. The finer portions of the sediments contain a well preserved faunal assemblage. The mixture of foraminifers like *Ammonia parkinsoniana* sp. and ostracoda like *Ilyocypris bradyi* Sars (1890) in the same sediment samples indicates superposition of environments varying from marine/brackish to fresh water. Particularly, *Ilyocypris bradyi* is generally thought to live in ponds, swamps, lakes, streams, and even ephemeral water bodies (Sokolov, 1989; Griffiths, 1995). Its stratigraphic range is Early Pleistocene - Holocene (Griffiths, 1995). A large amount of reworked planktonic and benthic faunas was also found within the sands, indicating a significant income from the surrounding Pliocene - Middle Pleistocene open-water marine sediments. The transition between coastal and fluvial deposits is widely exposed in the 7 metre-high walls of a large quarry near the Metauro River mouth, where it is marked by a gradual decrease in amount and thickness of gravel layers and corresponding increase of massive yellow sand.

Remnants of the third order terrace (*C3*) are widespread along the whole coastal belt but not well preserved. They have often been remodelled, which make the estimation of their inner edge elevation less accurate than in younger terraces. South of the Misa River mouth they have been totally eroded by widespread rock slides. The better preserved remnants are several hundred metre broad and have their inner edges at an elevation between 23 m and 40 m. The depositional body of the terrace is never clearly exposed but rounded flat pebbles, overturned by ploughing, are scattered all over the top surface of the terrace.

Numerous remnants of older coastal terraces are arranged in ribbons parallel to the coastline. They are generally a few hundred square metres large but heavily remodelled, and their depositional bodies are never exposed. Although they can be found all along the coastal slope, individual remnants generally lie a few kilometres apart and thus are difficult to correlate. Despite their subtle geologic/geomorphic expression, we could identify at least two more orders respectively culminating at 48 – 56 and 70 - 73 m. These ranges seem also in good accordance with those of older fluvial terraces at their lowermost reaches.

### 1.3.3. Fluvial terraces

The first order terrace (*F1*) was identified only in the central and northern part of the study area, whereas in the Misa and Esino valleys it appears not to have formed at all (**Figure 2**). It is consistently found entrenched within the older terraces, stretches almost continuously along both river sides and is generally well preserved. Along the lowermost reaches terrace treads can be up to ~1 km-wide. Terrace inner edge elevations generally range between 5 and 10 m above the present-day floodplain. The depositional body of the terrace is never clearly exposed because of dense urbanisation.

The second order terrace (*F2*) is very well preserved all throughout the study area; its tread surfaces are the most continuous and the largest among the various orders. Remnants on the north-western side of the valley are locally wider than 4 km and always broader than those on the opposite side. Terrace inner edge elevations generally range between 10 and 40 m above the present-day floodplain. The depositional body of this terrace is well exposed only in the valley of the Metauro River. Main exposures include one in the active quarry near the river mouth (already mentioned in the description of C2) and another in a dismissed quarry located 8 km upstream. In the latter, the 7 m-high exposed wall is topped by a 40 cm-thick brown soil lying over poorly sorted, rounded, and imbricated gravels with 20-30 cm-thick, less than 10 m-wide sand lenses. The gravels are essentially derived from Meso-Cenozoic carbonate rocks with rare dark flint and yellowish sandstone pebbles. Bedding is mostly planar, however, sandy-pebbly bodies with cross-bedding strata occur locally.

The third order terrace (*F3*) was also identified throughout all six main valleys of the study area. Its remnants are almost continuous and fairly well preserved in the lower-middle reaches, where they are up to 0.5 km-wide. Terrace inner edge elevations generally range between 20 and 70 m above the present-day floodplain. The terrace sedimentary body is never well exposed, however, some alluvial deposits are seen in minor building-site excavations and inferred from the presence of scattered rounded pebbles in ploughed fields.

Remnants of older fluvial terraces were identified in all river valleys, though their majority was preserved only on the north-western side of each. Despite their rareness and bad state of preservation, we reconstructed three more terrace orders whose treads lie between 50 and 190 m above the present-day floodplain. In most valleys they were found only within 10 km of the coast. Their sedimentary bodies could not be observed in the field due to missing exposures, so that they can either be considered as strath terraces or aggradational terraces that were largely stripped of their deposits.

### 1.3.4. Local drainage anomalies

Following is a summary of local anomalies of the current drainage system and of its fossil counterparts, separated into two groups and keyed to symbols in **Figure 2**. The first group includes anomalies that were recognised in map view, i.e. anomalies in the expected horizontal trend of the channel (horizontal anomalies); the second includes those that were detected in river profiles, i.e. anomalies in the expected height or depth of downcutting of the channel (vertical anomalies).

*Horizontal anomalies*

(H1) In its lowermost reach 4-10 km from the coastline the Metauro River makes a wide right turn towards the south-eastern side of its valley, where it is entrenched into its own alluvial plain.

(H2) At ~5.5 km from the coastline the Metauro River channel undermines the south-eastern wall of Pliocene marine bedrock.

(H3) The Cesano River channel seems to have been forced to sweep south-eastward ~3 km from its mouth, where it also undermines the Pliocene bedrock of its southern valley flank.

*Vertical anomalies*

(V1) Between 3.5 and 8 km upstream from the mouth the northwestern side of the Metauro Valley is draped by minor terrace treads, located on the riser between *F1* and *F2*. In the same area, the top surface of *F2* has a strong gradient upslope perpendicular to the river course.

(V2) The Misa River is presently incising all along its course, even as it approaches the coastline.

(V3) Entrenched meanders of minor river courses, such as the Tavollo, Ventena, Arzilla and some tributary streams, carve the top surface of *F1* and *F2* near the coastal-fluvial transition.

(V4) The Triponzio River, Rubiano Stream, and other minor streams incise the top surface of *F1* and *F2* in the Esino basin.

(V5) In its last kilometre before the mouth the Conca River still seems to be more prone to incising than discharging its deposits.
(V6) The Foglia River channel switches from aggradational to degradational behaviour in its lower alluvial plain 8 km from the mouth.
(V7) Farther upstream in the Foglia valley, between 10 and 14 km from the mouth, there are several depositional remnants at 1-4 m above the present floodplain and below *F1*.

### 1.3.5. Age of the terrace sequence

The lateral continuity of coastal terrace treads is a useful geomorphic property for correlating remnants of abandoned floodplains belonging to separate drainage basins. In our study area, the geomorphic correlation was largely helped by the very good preservation of bevelled terrace treads that continue seamlessly at the transition from the riverine to the coastal plain. Room for major uncertainties is then left only for the older and less preserved terraces, whose remnants may fall several kilometres apart. Classical correlation through the analysis of sedimentary logs in this area proved almost impossible. First because the dense urbanisation conceals the natural exposures of sediments. Second because quarrying activities were outlawed long ago, preventing deposits from being artificially exposed. However, the analysis of the few available exposures, along with the scrutiny of overturned shallow sediments in field furrows, allowed the composition of terrace deposits to be determined with sufficient confidence.

The whole suite of coastal and estuarine terraces can be framed between the age of its marine substratum and Present. The Pliocene-Pleistocene sandy-silty marine sequence crops out widely in the area. Cantalamessa et al. (1986) constrained both the Miocene/Pliocene and Pliocene/Pleistocene boundaries through benthic and planktonic faunal markers and indicated that the Early/Middle Pleistocene boundary (780 ka) lies within a coarse conglomerate on top of the sequence. This deposit also marks the transition from marine to continental environment (Cantalamessa et al., 1986). The fluvial/coastal terrace sequence, therefore, is younger than 780 ka because it develops entirely within deep valleys carved into the marine depositional body. Considering that the terrace sequence is made up by a total number of six/seven orders, and assuming that it had developed continually, the main terrace orders should have formed at major (~ 100 ka) eustatic cycles. Minor terraces, instead, should have formed at minor base level fluctuations.

Positively documented 125-ka coastal terrace remnants (created during the Oxygen Isotope Stage 5e) are generally the widest and best preserved in any given flight of terraces (for Italy see Bordoni and Valensise, 1998, and references therein). This is likely to result from the longer duration of this high stand combined with the higher elevation reached by sea-level (+6 m) with respect to later stands. Studies of the 125-ka terraces and deposits flourished in Italy and the Mediterranean as early as the beginning of the XX century thanks to the widespread occurrence of index fossil *Strombus Bubonius* LMK. This circumstance allowed a detailed reconstruction of the 125-ka strandline throughout most of central and southern Italy. According to Selli (1962) and later investigators, however, the Adriatic Sea never experienced the warmer conditions that favoured the northward migration of warm fauna such as *Strombus Bubonius*, which has never been reported north of Puglia.

Based on the geomorphic evidence outlined above and on the lack of absolute nor stratigraphic dating of the reconstructed terrace sequence, we tentatively correlated *C2*, consistently the best preserved terrace of the sequence, with the 125-ka sea level high stand. *C3* might thus be correlated with the ~212-ka high stand (stage 7), while *C1* remains undetermined.

## 1.4. Tectonic interpretation of geomorphic data

Our basic approach to interpret the tectonic control on the formation of the terrace sequences is to examine the spatial pattern of their elevations. We rely on the assumption that terrace treads were constructed and maintained as the active river and coastal floor during periods of sea level high stands, and then abandoned and dissected during periods of sea level fall. Therefore we sampled the inner edge elevation of all identified terrace remnants from topographic maps (1:25,000 and 1:10,000 scale), reconstructed continuous strandlines, and plotted them onto profiles parallel to the shoreline and to river valley axes. **Figure 3** shows the elevations of the first three younger orders of coastal terraces projected along the present shoreline (*C1*, *C2*, *C3),* including elevations inferred from the downstream trend of fluvial terrace treads. A closer inspection reveals that *C1*, *C2* and *C3* vary their relative elevations and vertical separations following a systematic pattern. A major elevation change occurs between the mouths of the Conca and Foglia Rivers, however, the scarcity of terrace remnants prevents a more detailed analysis. South of the Foglia River, the three terraces are nearly horizontal up to near the Misa River mouth, where the first order disappears and the elevations of the second and third orders drop abruptly. South of the Misa, the elevations of *C2* and *C3* rise again and then gradually decrease.

**Figure 4** shows the elevation of the first principal three younger orders of fluvial terraces (*F1*, *F2*, *F3)* projected along mid-valley axes for all six analysed rivers. These profiles include the elevation of correlative coastal terraces, where known. To analyse the shape of elevation profiles and verify if any systematic pattern exists, we first geometrically fitted the elevation points of present-day alluvial plains with a simple concave-up curve of the form $Y = a + b\ X^{**}c$. Then, by varying $a$ and $b$, we shifted the curve upward to fit the elevation points of terrace remnants. By doing so we have been able to (1) gauge the amount of vertical separation between terrace treads along river and verify that they converge downstream, (2) predict where the point of convergence is located, and (3) detect possible departures from the average trend. The adoption of this curve, however, rests on the assumption that the valleys where the older terraces formed had the same downstream curvature as the present-day alluvial plain.

The Conca and Cesano River valleys have the steepest grade while the other rivers average about the same (**Figure 4**). The grade of reconstructed terrace treads varies accordingly. All terraces converge downstream independently of the grade. The vertical separation between *C3* and *C2* is always greater than that between lower orders. On the basis of the rate of convergence, we estimated that the point of intersection of the Conca valley terraces falls near the coast, while that of the other valleys lies offshore: between 10 and 20 km for Foglia, Metauro, and Cesano, about 5 km for Misa and Esino.

As clearly pointed out by Keller and Pinter (2002), simple downcutting in a river valley subjected to homogeneous uplift would lead to a sequence of parallel terraces, while downstream convergent patterns require tectonic tilting (i.e., differential uplift). Following this scheme and considering that downstream convergence was observed in all the studied river valleys, we inferred that the amount of uplift of the frontal slope of the Apennine accretionary prism tapers north-eastward and nulls at the point of convergence. In other words, at least during the time interval spanned by the fluvial terraces, the whole area has been undergoing tectonic tilting about a NW-SE axis located somewhere between the coast and about 20 km offshore. If our assignment of *C2* to the 125-ka high stand holds true, the uplift rate at the coastline would be 0.1 mm/y at the most. Assuming that the variation of vertical spacing between fluvial terraces is proportional to the variation of uplift, one obtains an uplift rate at the Apennine regional divide (about 60 km inland) in the range 0.5-1.0 mm/y, in agreement with estimates obtained from other lines of geological and geomorphic evidence (~0.5 mm/y: Dramis, 1992; 1-2 mm/y, Bigi et al., 1997).

**Figure 4** also shows that the data points of fluvial terrace treads sometimes follow an undulated pattern above and below the best-fit curve. Of special interest are the fluctuations of the younger terraces in the lowermost valley reaches, that all show a remarkable convex-up shape within the first 10 km upstream from the mouth. These geomorphic features suggest that crustal displacement affects the study area also at a local scale of a few kilometres. This short-wavelength warping is well explained by the activity of the anticlines that lie along the coastal belt (**Figure 2**). These have long been known for they are mapped in the official geological maps (Italian Geological Survey, scale 1:100,000)

and have been probed through shallow and deep wells and geophysical prospecting (Bally et al., 1986; Nanni and Vivalda, 1987; De Donatis et al., 1998). Notice that for all six rivers the point of maximum terrace up-warping closest to the coast coincides within 1-2 km with the axes of these anticlines (shown by arrows in **Figure 4**).

Since the deformed alluvial terraces are extremely youthful geological features, we interpret the warping process as active. This is also supported by the anomalous behaviour of rivers near the coast (see **Figure 2**): the abrupt change from aggradational to degradational behaviour of the Foglia River (anomaly **V6**); the presence of entrenched meanders in the lowermost reaches of all rivers; and the systematic lateral migration of river channels. This evidence also suggests that a ~10 km-wide ribbon along the coast is being raised at a faster rate relative to the adjacent inland areas. **Figure 5** shows qualitatively the geomorphic and sedimentological response to progressive growth of the coastal anticline along the Foglia River. The test is based on standard dislocation modelling of slip on a buried fault embedded in an elastic half-space. Fault geometry and size are constrained by the subsurface images supplied by Bally et al. (1986) and De Donatis et al. (1998). Zones of expected maximum uplift and subsidence coincide with areas of stream incision and sediment accumulation, respectively. Notice that the horizontal separation between these two maxima is strictly proportional to the width of the model fault (and, to a lesser extent, to its dip). A substantially thinner (shallower) or wider (deeper) fault would respectively predict a smaller and larger separation between the two anomalous areas than it is observed in the field.

We conclude that the growth of the coastal anticlines is driven by sustained slip at depth on the underlying blind-thrust faults. If this conclusion is correct, we can use dislocation modelling to predict tentatively the fault slip rate needed to generate the observed short-wavelength terrace warping. For terrace *F2*, for which we assumed an age of ~125 ky, the vertical separation between the uplifting convexity and the subsiding trough is 10-15 m on average. Depending on fault geometry, a total slip of 30-45 m is required to produce this amount of surface displacement, corresponding to a slip rate of 0.24-0.36 mm/y.

The main tectonic features above illustrated fit in a comprehensive model of active mountain range development (**Figure 6**) where tectonic processes operate at two different wavelengths (~100 km and ~10 km) and interact with the geomorphic sculpting of the land surface. Notice that the area of local warping extends well off the coast and that at least another alignment of blind faults is buried in the near offshore, as suggested by deep geophysical evidence (Bally et al., 1986; De Donatis et al., 1998). This area also coincides with that affected by major seismic release. All together these observations strongly suggest that the thrust faults are responsible for the largest earthquakes of the area: first, because based on current relationships between fault size and earthquake magnitude (Wells and Coppersmith, 1994), the length of the faults that drive the anticlinal growth well matches the size of the faults expected to have originated the largest earthquakes (see also **Figure 5**); second, because the limited but sudden up-warping of sea-floor that they may produce during an earthquake explains the record of tsunami associated with historical earthquakes (**Table 1**).

## 1.5. Discussion: tectonic significance and seismogenic implications

The identification of coastal terraces in the northern Marche area is one of our main results. Our work extends data previously gathered outside the study area. For example, Parea and Valloni (1983) identified coastal terraces 120 km south of Ancona, while Parea (1986, 1987) described Middle-Late Pleistocene coastal deposits in the area north of Rimini and correlated them with eustatic highstands. Our new findings provide (1) a reference to correlate terraces across neighbouring river basins; (2) a proxy for correlating terrace treads with past sea levels; (3) the evidence of coastal tectonic uplift; and (4) the possibility of calculating rates of uplift and hence rates of slip of the faults driving it.

We also verified that river terraces converge downstream systematically and that terrace treads are significantly warped in the proximity of the coast. Lipparini (1939) first noticed this large-

scale feature in some drainage basins of the area and proposed that it "*indicates an uplift ... more active in the Apennines than toward the sea*". Later on, Elmi et al. (1987) proposed that the point of river convergence indicates the transition between uplifting and subsiding areas. On the basis of a geometric reconstruction of the erosion surface buried beneath the alluvial deposits and observations on the migration of river channels, Nanni and Vivalda (1987) also suggested that the fluvial network might be controlled by tectonic activity. In their view, NE-SW trending faults would control the general drainage pattern, whereas minor northward channel migrations near the coast would be driven by a NW-SE growing anticline. Based on the analysis of alluvial terraces of the Metauro and Foglia valleys, Nesci et al. (1990) also suggested that "*generalised tectonic uplift ... interacts with minor differential tectonic movements indicated by local convergent and divergent* [i.e. warped) *terraces*".

As discussed above, our tectonic scheme moves along the same line as the interpretations of previous authors. However, we brought forward the following new facts:

(1) we combined regional- and local-scale tectonic deformations into a single kinematic model that applies to a larger area;
(2) proposed that local scale deformation can be due to active blind thrust faults that drive the growth of the coastal anticlines;
(3) suggested that such blind thrusts can be responsible for the largest earthquakes of the region;
(4) provided a new basis for assessing the seismic hazard of the region.

The first two points deal strictly with the tectonic interpretation of geomorphic features that was illustrated in the previous section. Conversely, the third and fourth points deal with the unavoidable implications in terms of seismogenic behaviour of faults. We believe they deserve to be elucidated in better detail.

Our tectonic interpretation bears the intrinsic consequence that, apart from minor spatial and temporal fluctuations, the entire thrust front is active. Knowing that several parts of it were characterised by stick-slip behaviour in the recent past (that is to say, they generated earthquakes), we believe it reasonable to infer that the rest of the thrust system will probably do likewise. In other words, we believe the entire thrust front should be considered potentially seismogenic, a rather conservative but realistic working hypothesis. Further work is needed to assess how much of the fault displacement is spent in earthquake preparation and how much is consumed in earthquake-free stable-sliding processes.

The historical record of the northern Adriatic coast brings out another incumbency for the earthquake geologist. Consider that the thrust system has the following properties:

- geological and geophysical surveys suggest that it extends seamlessly all along the coast;
- our work supplied ample evidence that it is active for its entire length;
- during the past four centuries it released several earthquakes in the M range 5 to 6 (see **Table 1**), all lined-up along the coast a few kilometres apart;
- as suggested also by previous workers, the system is crossed by transverse tectonic lineaments that break it up in 10-15 km individual fault segments, each capable of releasing a M 5.5+ earthquake.

Standard empirical relationships between earthquake magnitude and fault size (e.g. Wells and Coppersmith, 1994) show that the cumulative length of faults that ruptured in known earthquakes is much shorter than the total length of the thrust system. Notwithstanding the uncertainties that still exist on the exact assignment of each historical earthquake to a specific seismogenic source (discussed in Basili, 2001, and Basili and Valensise, 2001), there are certainly a few ~10 km-long "empty spaces" along the Adriatic thrust system. If the corresponding fault segments have the same mechanical/frictional properties as their neighbours, they may be considered as potential seismic gaps. Current seismic hazard of selected areas of northern Marche could therefore be substantially higher than currently estimated based on seismicity rates and standard Poisson-type approaches (e.g. Albarello et al., 1999).

## 1.6. References

Albarello, D., Bosi, V., Bramerini, F., V. Lucantoni, A., Naso, G., Peruzza, L., Rebez, A., Sabetta, F. and Slejko, D., 1999, New seismic hazard maps of the Italian territory: available from (http://www.serviziosismico.it/PROG/2000/carte_pericolosita/).

Amato, A. and Cocco, M. (eds) 2000, Special issue: The Umbria-Marche, central Italy, seismic sequence of 1997-1998, *J. of Seismology*, 4(4), 333-612.

Arvidsson, R. and Ekström, G., 1998, Global CMT Analysis of Moderate Earthquakes Mw 4.5 using Intermediate Period Surface Waves, *Bull. Seism. Soc. Am.* **88**, 1003-1013.

Bally, A.W., Burbi, L., Cooper, C. and Ghelardoni, R., 1986, Balanced sections and sesmic reflection profiles across the central Apennines, *Mem. Soc. Geol. It.* **35**, 257-310.

Barba, S. and Basili, R., 1999, Analysis of seismological and geological observations for moderate size earthquakes: the Colfiorito Fault System (Central Apennines, Italy), *Geophys. J. Int.* **141**, 241-252.

Baroux, E., Pino, N.A., Valensise, G., Scotti, O. and Cushing, M., 2003, Source parameters of the 11 June 1909, Lambesc (southeastern France) earthquake: a re-appraisal based on macroseismic, seismological and geodetic observations, *J. Geophys. Res.*, in press.

Basili, R., 2001, Seismogenic sources from Geologic/Geophysical Data: 29-Conero Offshore, 30-Senigallia. In: Valensise, G. and Pantosti, D. (eds), 2001, *Database of Potential Sources for Earthquakes Larger than M 5.5 in Italy*, Annali di Geofisica, Suppl. to vol. 44(4), 180 pp.

Basili, R. and Valensise, G., 2001, Seismogenic sources from Geologic/Geophysical Data: 31-Fano Ardizio, 32-Pesaro San Bartolo, 33-Rimini Offshore South, 34- Rimini Offshore North, 35-Rimini, 36-Val Marecchia. In: Valensise, G. and Pantosti, D. (eds), 2001, *Database of Potential Sources for Earthquakes Larger than M 5.5 in Italy,* Annali di Geofisica, Suppl. to vol. 44(4), 180 pp.

Benedetti, L., Tapponier, P., King, G.C.P., Meyer, B. and Manighetti, I., 2000, Growth folding and active thrusting in the Montello region, Veneto, northern Italy, *J. Geophys. Res.* **105,** B1, 739-766.

Bigi, S., Centamore, E. and Nisio, L., 1997, Elementi di tettonica quaternaria nell'area pedeappenninica marchigiano-abruzzese, *Il Quaternario*, **10**, 359-362.

Bordoni, P. and Valensise, G., 1998, Deformation of the 125 ka marine terrace in Italy: tectonic implications. In: Stewart, I. and Vita-Finzi, C. (eds), 1998, *Coastal Tectonics*. Geol. Soc. London Spec. Pub., **146**, 71-110.

Boschi, E., Guidoboni, E., Ferrari, G., Mariotti, D., Valensise, G. and Gasperini, P., 2000, Catalogue of Strong Italian Earthquakes, 461 b.C. to 1997, *Annali di Geofisica* **43**(4), 609-868, with database on CD-ROM.

Burrato, P., Ciucci, F. and Valensise, G., 2003, River response to blind thrust faulting in the Po Plain, northern Italy, *Annals of Geophysics*, in press.

Cantalamessa, G., Centamore, E., Chiocchini, U., Colalongo, M.L., Micarelli, A., Nanni, T., Pasini, G., Potetti, M., Ricci Lucchi, F., Cristallini, C. and Di Lorito, L., 1986, Il Plio-Pleistocene delle Marche. In: Centamore, E. and Deiana, G. (Eds), *La Geologia delle Marche*. Studi Geologici Camerti, Num. Spec., 61-81.

Coward, M.P., De Donatis, M., Mazzoli, S., Paltrinieri, W. and Wezel, F.C., 1999, Frontal part of the northern Apennines fold and thrust belt in the Romagna-Marche arc (Italy): shallow and deep structural styles, *Tectonics* **18**, 3, 559-574.

De Donatis, M., Invernizzi, C., Landuzzi, A., Mazzoli, S. and Potetti, M., 1998, Crop 03: structure of the Montecalvo in Foglia-Adriatic sea segment, *Mem. Soc. Geol. It.* **52**, 617-630.

Di Bucci, D. and Mazzoli, S., 2002, Active tectonics of the Northern Apennines and Adria geodynamics: new data and a discussion, *Journal of Geodynamics* **34**, 687-707.

Doglioni, C., Mongelli, F. and Pialli, G., 1998, Boudinage of the Alpine Belt in the Apenninic back-arc, *Mem. Soc. Geol. It*. **52**, 457-468.

Dramis, F., 1992, Il ruolo dei sollevamenti tettonici a largo raggio nella genesi del rilievo appenninco, *Studi Geol. Camerti*, spec. vol. 1992/1, 9-15.

Elmi, C., Nesci, O., Savelli, D. and Maltarello, G., 1987, Depositi alluvionali terrazzati del margine adriatico appenninico centro-settentrionale: processi geomorfologici e neotettonica, *Boll. Soc. Geol. It.* **106**, 717-721.

Elter, P., Giglia, G., Tongiorgi, M. and Trevisan, L., 1975, Tensional and compressional areas in the recent (Tortonian to present) evolution of the Northern Apennines, *Boll. Geof. Teor. Appl*. **17**, 3-18.

Frepoli, A. and Amato, A., 1997, Contemporaneous extension and compression in the Northern Apennines from earthquake fault-plane solutions, *Geophys. J. Int*. **129**, 368-388.

Griffiths, H.I., 1995, *The application of freshwater Ostracoda to the reconstruction of Late Quaternary Palaeoenvironments in North-western Europe*, PhD Thesis, University of Wales, 449 pp.

Gruppo di Lavoro CPTI, 1999, *Catalogo Parametrico dei Terremoti Italiani*, I.N.G.-G.N.D.T.-S.G.A.-S.S.N., Bologna, 88 pp.

Keller, E.A. and Pinter, N., 2002, *Active tectonics: earthquakes, uplift, and landscape*, Prentice Hall, New Jersey, 362 pp.

Keller, E.A., Zepeda, R.L., Rockwell, T.K., Ku, T.L. and Dinklage, W.S., 1998, Active tectonics at Wheeler Ridge, southern San Joaquin, California, *Geol. Soc. Am. Bull*. **110**, 298-310.

Lavecchia, G., Brozzetti, F., Barchi, M., Menichetti, M. and Keller, J.V.A., 1994, Seismotectonic zoning in east-central Italy deduced from an analysis of the Neogene to present deformations and related stress fields, *Geol. Soc. Am. Bull*. **106**, 1107-1120.

Lipparini, T., 1939, I terrazzi fluviali delle Marche, *Giorn. Geol*. s. 2 **13**, 5-22.

Montone, P., Amato, A. and Pondrelli, S., 1999, Active Stress Map of Italy, *J. Geophys. Res.* **104**, B11, 25595-25610.

Nanni, T. and Vivalda, P., 1987, Influenza della tettonica trasversale sulla morfogenesi delle pianure alluvionali marchigiane, *Geogr. Fis. Din. Quat*. **10**, 180-192.

Nesci, O., Savelli, D. and Mengarelli, D., 1990, I terrazzi vallivi del 1° ordine nei bacini dei Fiumi Metauro e Foglia (Appennino marchigiano), *Geogr. Fis. Din. Quat*. **13**, 63-73.

Parea, G.C., 1986, I terrazzi marini tardo-pleistocenici del fronte della catena appenninica in relazione alla geologia dell'avanfossa adriatica, *Mem. Soc. Geol. It*. **35**, 913-936.

Parea, G.C., 1987, Paleogeografia e tettonica tardo-pleistoceniche del pedeappennino modenese, *Mem. Soc. Geol. It*. **39**, 433-446.

Parea, G.C. and Valloni, R., 1983, Le paleospiagge pleistoceniche della zona di Atri-Silvi (Abruzzo), *Atti Soc. Nat. Mat.*, Modena, **114**, 51-82.

Philip, H., Bousquet, J.C., Escuer, J., Fleta, J., Goula, X. and Grellet, B., 1992, Présence de failles inverses d'âge quaternaire dans l'Est des Pyrénées: implications sismotectoniques, *R. Acad. Sci. Paris* **314**, Sér. II, 1239-1245.

Pondrelli, S., Morelli, A., Ekström, G., Mazza, S., Boschi, E. and Dziewonski, A.M., 2002, European-Mediterranean regional centroid-moment tensors: 1997-2000, *Phys. Earth Planet. Int*. **130**, 71-101.

Rockwell, T.K., Keller, E.A. and Dembroff, G.R., 1988, Quaternary rate of folding of the Ventura Avenue anticline, western Transverse Ranges, Southern California, *Geol. Soc. Am. Bull*. **100**, 850-858.

Savelli, D., De Donatis, M., Mazzoli, S., Nesci, O., Tramontana, M. and Veneri, F., 2002, Evidence for Quaternary Faulting in the Metauro River Basin (Northern Marche Apennines), *Boll. Soc. Geol. It*. Vol. Spec. 1, 931-937.

Scientists of the U. S. Geological Survey and the Southern California Earthquake Center, 1994, The magnitude 6.7 Northridge, California, earthquake of January 17, 1994, *Science* **266**, 389-397.

Sebrier, M., and SAFE Consortium, 2003, Active faulting in low- to moderate-seismicity regions: the SAFE European project, presented at the EGS AGU EUG Joint Meeting, Nice 6-11 April 2003 (abstract).

Selli, R., 1962, Le quaternarie marin du versant Adriatique-Ionien de la péninsule italienne, *Quaternaria,* **6**, 391-413.

Shaw, J.H. and Shearer, P.M., 1999, An elusive blind-thrust fault beneath metropolitan Los Angeles, *Science* **283**, 5407, 1516-1518.

Sokolov, B.S. (ed.), 1989, *Prakticheskoje rukovodstvo po mikrofaune SSSR, Tom 3, Ostrakody kajnozoja*, Ministerstvo geologii SSSR, Nedra Leningradskoje otdelenije, Leningrad, 236 pp.

Stein, R. and Ekström, G., 1992, Seismicity and geometry of a 110-km-long blind thrust fault; 2, Synthesis of the 1982-1985 California earthquake sequence, *J. Geophys. Res*. **97**, B4, 4865-4883.

Valensise, G. and Pantosti, D. (eds), 2001, Database of Potential Sources for Earthquakes Larger than M 5.5 in Italy, *Annali di Geofisica*, Suppl. to vol. 44(4), 180 pp., with CD-ROM.

Valensise, G. and Pantosti, D., 1992, A 125-kyr-long geological record of seismic source repeatability: the Messina Straits (southern Italy) and the 1908 earthquake (MS 7 1/2), *Terra Nova* **4**, 472-483.

Ward, S.N. and Valensise, G., 1996, Progressive growth of San Clemente Island, California, by blind thrust faulting: implications for fault slip partitioning in the California Continental Borderland, *Geophys. J. Int*. **126**, 712-734.

Wells, D.L. and Coppersmith, K.J., 1994, New Empirical Relationships among Magnitude, Rupture Length, Rupture Width, Rupture Area, and Surface Displacement, *Bull. Seism. Soc. Am*. **84**, 974-1002.

***Figure 1*** *- Sketch-map of the northern Marche and surrounding areas with the focal mechanisms of the 1987 Porto S. Giorgio earthquake (Montone et al., 1999) and of the 2000 Forlì sequence (Pondrelli et al., 2002).* Square*: historical earthquake (Gruppo di Lavoro CPTI, 1999);* arrow*: locality were a tsunami was observed (Boschi et al., 2000; numbers labelling both squares and arrows refer to earthquakes of Table 1);* dashed line*: regional drainage divide;* hachured line*: Apennine outermost thrust front;* solid line segment*: minimum horizontal stress axis from borehole breakout data (Montone et al., 1999).*

***Figure 2*** *- A) Sketch-map of the northern Marche region.* Dark-grey ribbon*: coastal anticline axis;* light-grey area*: outcrop of pre-Pliocene bedrock;* Hn and Vn*: horizontal and vertical drainage anomalies (see text for explanation);* double-headed arrow*: convex-up shaped fluvial terrace. B) 3D view of the Northern Marche piedmont with the Apennine Range at the back as seen from the North.*

***Figure 3*** *- Profile of the inner edge elevation of coastal terraces projected along the coastline.* Solid symbol*: observed elevation;* open symbol*: elevation inferred from the correlative fluvial terrace;* square*: first order terrace* C1*;* circle*: second order terrace* C2*;* diamond*: third order terrace* C3*;* triangle*: river mouth;* shaded band*: areas where terraces are not preserved.*

***Figure 4*** *- Profiles of the inner edge elevation of fluvial terraces for the six analysed rivers, projected along mid-valley axes.* Solid symbol*: observed elevation;* open symbol*: elevation observed on the correlative coastal terrace;* square*: first order terrace* F1*;* circle*: second order terrace* F2*;* diamond*: third order terrace* F3*;* dashed line*: best-fitting curve;* arrow*: river intersection with the axis of coastal anticline.*

***Figure 5*** *– Elastic dislocation modelling of the expected geomorphic and sedimentological response to progressive growth of the coastal anticline along the Foglia River. Modelling assumes unitary slip on a blind thrust fault embedded in an elastic half-space. Contours of expected vertical displacement (expressed as a fraction of slip) highlight the zone of maximum uplift and subsidence. Notice that the river discharges most of its sediment load in the area of maximum subsidence. It then continues its run toward the sea and crosses the anticline with a renewed power wearing down the alluvial plain.*

***Figure 6*** *- Comprehensive model of active tectonics in the Apennines frontal prism (approximate scale). Rates of regional uplift and tilting are those inferred from the downstream convergence of fluvial terrace treads (see text). Fault slip rate was derived from the estimated age*

*and extent of warping of the second order terrace through elastic dislocation modelling (see text).*

**Table 1** - Historical earthquakes (Me>5) of the northern Marche coastal belt and surrounding areas (Gruppo di Lavoro CPTI, 1999) and associated tsunami reports (Boschi et al., 2000).

| ID | Date | Me | Io | Locality affected by tsunami | Tsunami effects |
|---|---|---|---|---|---|
| 1 | 14 Apr 1672 | 5.7 | VIII | Rimini | First wave: withdraw. Inundation: 15 m |
| 2 | 23 Dec 1690 | 5.5 | VIII-IX | Ancona | First wave: withdraw. Boats scarred on sea bed |
| 3 | 25 Dec 1786 | 5.7 | VIII | No record | No record |
| 4 | 17 Mar 1875 | 5.8 | VIII | Rimini, Pesaro, Ancona, Cervia, Cesenatico | Generic |
| 5 | 17 May 1916 | 5.7 | VIII | Retinella | Generic |
| 6 | 16 Aug 1916 | 5.6 | VIII | Mouth of Tavollo River | Generic |
| 7 | 02 Jan 1924 | 5.2 | VII-VIII | Senigallia | Uncertain record |
| 8 | 30 Oct 1930 | 5.9 | IX | Ancona | Harboured steamship broke the moorings |
| 9 | 14 Jun 1972 | 5.2 | VIII | Ancona | Uncertain record |

# Section 2 – The Mantova-Mincio River area (central Po Plain)

**by Antonella Astori**

## *2.1. Introduction*

Several fluvial and topographic anomalies occur in the central Po Plain. One of the most evident is near Mantova and corresponds to the sharp eastward deflection of the River Mincio and the presence of a lake along its course. Previous studies supposed a tectonic control on the evolution of the Mincio area (Baraldi et al., 1980; Arca e Beretta, 1985; Castaldini and Panizza, 1988; Serva 1990; Castaldini and Panizza, 1991; De Martini et al., 1998; Burrato et al., 1999; Valensise and Pantosti, 2001). The most recent of these hypotheses, based on geodetic and geomorphic literature, assume that the anomalies and the geomorphological evolution of this part of the Po Plain are the result of slipping on a south-verging north-dipping buried thrust fault.

As similar geomorphic anomalies in nearby areas have already been positively correlated with well expressed buried anticlines, aim of this study is the geomorphological and topographic analysis of the surface in order to improve the knowledge of the geometry, kinematics and slip-rate of this hypothesised fault. Geomorphological features have been investigated by the means of historical maps, remote sensing, microrelief analysis and field surveys; the result is that the "Mantova anomaly" can be explained without involving active tectonic structures, which anyway do not find evidence.

## *2.2. Geological setting and Po Plain evolution*

The Po Plain is the most extensive plain in Italy (46,000 km$^2$) and it is the western emerged part of the Adriatic Sea sedimentary basin. It is located between the Southern Alps south-verging thrusts and north-verging Apennine structures, therefore it has been the foreland and then the foredeep of two opposite verging chains.

Geological knowledge of the Po Plain widely comes from seismic lines and hydrocarbon exploration drillings of the Eni Divisione Agip dataset (Carcano and Piccin, 2002; Pieri and Groppi, 1981; Cassano et al., 1986). From Oligocene onwards the Po Plain became an active continental margin; here took place the development of two syn-orogenic molasse basins, the older one linked to the Alps and the subsequent one (after Messinian) to the Apennines.

In Upper Miocene, most of the south-Alpine margin and parts of the plain emerged. They were subjected to deep erosion during Messinian, until a new marine transgression occurred in Pliocene.

Throughout Pliocene compressive tectonics acted along the Northern Apennines margin and submarine imbricated structures developed. This activity reduced in Quaternary when subsidence prevailed in the whole Po Plain.

Up to Pleistocene, the sea held the Po basin and since Early Pleistocene, continental sediments have progressively filled it in.

At 1.6 Ma, the slope-basin transition matched the south-Alpine margin between Lake Maggiore and Lake Garda. Until 0.8 Ma, the Alpine river fan-deltas and the Po delta system filled up

the western part of the basin: the slope-basin transition placed close to Brescia and extended eastward along the Alpine margin through the upper reach of River Mincio. Between 0.8 Ma and 0.6 Ma took place the last main northward shifting of the Apennine Folds, producing lower subsidence and therefore less room/space for the sediments entrained by both the Alpine and Apennine rivers. Their fan-deltas and the Po delta system merged and their sediments filled the deep basin entirely. At the same time, a global environmental change occurred, which is pointed out by two stratigraphic markers recognisable in the seismic profiles (Carcano and Piccin, 2002). Constant strong subsidence affected the Po Basin from 0.6 Ma onward, in the meantime, only minor uplift involved the Apennine structures and several global climate fluctuations drove the erosional and depositional processes.

## 2.3. Tectonic setting and seismicity

The central Alpine margin is a simple E-W trending structure gently dipping southwards (*Pede-Alpine Monocline*), while the northern Apennine margin is a more articulated structure (*Buried Apennine Front*): it is generally verging towards NNE and it extends in the subsurface of the plain arranged in three large arcs developed at different times.

The Mantova plain lies on the buried *Pede-Alpine Monocline*, but it is at the connection area among different systems: the E-W trend of the pede-Apennine arcs, the E-W trend of the South-Alpine buried front and the NNW-SSE trend of the Giudicarie system. Post-Tortonian released residual stress and/or active tectonics could be the cause of the most recent deformations locally known in these areas.

Concerning the seismological setting, the Po Plain is traditionally considered a low seismicity region. Most of the earthquakes listed in current historical catalogues are concentrated south of River Po along the pede-Apennines thrust front and on some buried Apennines outer fronts. North of River Po earthquakes are more infrequent and do not follow a regular pattern, but they are concentrated mainly in the pede-Alpine margin between Brescia and Verona.

## 2.4. Geomorphological setting

The Po Plain is bordered to the north by the Alps and to the south by the Northern Apennines. It is drained by the River Po, the longest italian stream (652 km), flowing from west to east toward the Adriatic Sea. The Alpine tributaries of River Po flow from north to south and they drain many mountains higher than 3.600 m a.s.l., where mainly carbonate, magmatic and metamorphic rocks outcrop. The Apennine tributaries run from north to south, they are shorter than the Alpine ones and drain mountains not higher than 2.200 m a.s.l., where clays, sandstones and marls are prevailing.

The northern and the southern sectors of the plain show several dissimilarities: they are different in the displayed geomorphic features, in sediment composition and above all, in the way and age of their formation (Figure 1). During the glacial ages, the Alpine glaciers reached several times the Po Plain. The paraglacial processes had a main role in the landscape evolution of the northern part of the plain, in spite of the southern sector, as only a few summits in the Apennines were covered by ice, which anyway did not reach the open plain. Moreover, the development of the northern sector of central Po Plain has been affected by the presence of deep Alpine lakes close to the plain.

In the study area the present-day main hydrography is in different way oriented: the River Chiese flows from north to south, the River Osone flows from NW to SE, the River Mincio from N to S until Grazie and from NW to SE downstream Mantova and the River Tione flows from NW to SE.

### *2.4.1 Lake Garda*

Lake Garda stays at 65 m a.s.l., it is the widest italian lake (370 km$^2$): its maximum length is 51.6 km and its maximum width is 17.2 km. The maximum depth is 346 m, therefore the lake bottom is under the today sea-level. The lake has only a main influent, the River Sarca, and only an effluent, the River Mincio.
The lake is narrow and elongate toward north and broad southwards, where a 100 km length morainic amphitheatre bounds it.

The Lake Garda shape and location are related to the presence of an important tectonic system (Giudicarie system, Figure 2) and to the moulding processes linked to the Pleistocene glaciations too.

The bedrock is 500 m deep in the northern part and 1259 m in the southern-most part, with a south-dipping bottom profile gradient (Fink, 1978).

After Bini et al. (1978), the origin of the depression of Lake Garda is related to an erosional phase induced by the drop in sea level during Late Miocene (Messinian), which acted along tectonically controlled directions. Later the deep canyon has been occupied by glaciers that therefore created not the depression, but followed the pre-Pliocene morphology.

### *2.4.2 The Garda morainic amphitheatre*

In the Lake Garda area five glacial stages have been recognised (Cremaschi, 1987): one in Early Pleistocene (Ciliverghe stage), three during Middle Pleistocene (M. Faita, Carpenedolo and Sedena stages) and one in Late Pleistocene (Solferino stage).
The moraines surrounding the Lake Garda are related to the Last Glacial Maximum (Solferino stage). The outer morainic ridge is the most elevated and the concentric inner ridges slope down toward the lake. Meltwater channels and kame separate them.
Outside the western part of the Garda morainic system, evidence of at least four previous glaciations exists.

During the last two glacial stages (Sedena and Solferino stages) the ice did not reached the sector west of River Chiese (Ciliverghe, Castenedolo, Gavardo, M. Faita), probably because of a tectonic uplift in Middle Pleistocene in that area, while the eastern sector was subsiding or at least subjected to lower uplift.

The temporal evolution of the Garda morainic system shows a progressive shifting eastwards of the subsequent ice tongues (Cremaschi, 1987). In fact, only in the western part the oldest glacial deposits outcrop and they were not covered by the most recent moraines, whilst in the eastern sector they would have been disrupted or buried by the more recent glacial advances/retreats.

### *2.4.3 River Mincio*

The River Mincio is located in central Po Plain, it is a left tributary of River Po and it is the only effluent of Lake Garda, the widest italian lake (370 km$^2$).

Along its course (75 km) many artificial channel diversions exist, so that the maximum discharge downstream Goito has been greatly cut down (from 200 $m^3$/sec to 70 $m^3$/sec; Baraldi and Zavatti, 1994) and therefore the nowadays-fluvial dynamics is strongly far from the natural pattern.

The River Mincio uppermost reach is entrenched in the hills of the Garda morainic amphitheatre. Downstream the hill foot, the river has moulded a large valley (up to 6 km in width) within the outwash plain sediments (Figure 3).

Being fed by a wide lake, River Mincio has generally steady flows and low sediment supply, having not an own catchment. Its tributaries are some resurgence watercourses flowing from NW, the main are Osone Vecchio, Seriola Marchionale, Seriola Birbesi, Scolo Caldone) and all of them rise at the foot central-western sector of the morainic amphitheatre hills.

The main peculiarity of River Mincio is the presence of a winding shallow lake in its middle reach (Mantova). The nowadays location of the lake is not natural: until about 1000 years ago it was not extended westwards, but was more lengthened toward the south (Figure 4) spreading between Porto Mantovano and Governolo, as stated by Marani (1967a, 1967b, 1969) on the basis of historical documents. During 1190, dykes were erected in the upper part of the lake; embankments were built in the southern part and the land reclaimed. During 1600, the lower boundary of the lake was at Formigosa, about 10 km upstream than the natural one. The present-day lake boundaries are 15 km upstream and 10 km westwards than the pristine location.

Another peculiarity is the sharp eastward deflection of the stream at Grazie: the riverbed changes the flow direction from N-S to W-E. About the reason of this turn, many authors assert that in former times, the River Mincio flowed southwards and only in VIII century b.C. (Veggiani, 1974) it shifted eastwards due to an outwash diversion explained as driven by active tectonic structures (Baraldi et al., 1980; Serva, 1990; Castaldini and Panizza, 1991; De Martin et al., 1998; Valensise and Pantosti, 2001).

The present study disagrees with this hypothesis. According to Baraldi and Pellegrini (1976), the paleo-channel downstream Grazie is correlatable better with the Osone paleo-drainage, while the Mincio was flowing far east than the present location.

## *2.5. Previous studies*

Many investigators described several anomalies in the Mantova area:

- eastward fluvial diversion and topographic anomaly related to the "Mantova anticline" supposed to be the expression of an active buried structure (Burrato et al., 2002; Valensise and Pantosti, 2001; De Martin et al., 1998);
- geochemical and piezometric anomaly with E-W direction just downstream Mantova lake (Castaldini and Panizza, 1991);
- Mincio diversion and sharp changes in subsurface lito-stratigraphic sequences N and S of Mantova lake (Serva, 1990; Baraldi et al., 1980);
- eastward fluvial diversion related to Mantova Line (Castaldini and Panizza, 1988);
- geodetic anomaly (Arca and Beretta, 1985);

To investigate these anomalies and particularly the "Mantova anticline", in addiction to the above-mentioned papers the literature concerning the following topics has been reviewed:

- geology (e.g.: Castellarin and Cantelli, 2000; Picotti et al., 1995; Doglioni, 1993; Sleiko et al., 1987; Castellarin and Vai, 1986; Ogniben, 1986; Castellari and Sartori, 1983; C.N.R., 1983; Zanferrari et al., 1982; Bini et al., 1978);
- Garda morainic amphitheatre and Mantova plain (Castiglioni and Pellegrini, 2001; Castiglioni et al., 1997; Cremaschi, 1987; Venzo, 1957; Nicolis, 1898);

- River Mincio paleochannels (Castaldini, 1989; Castaldini and Panizza, 1988; Baraldi and Pellegrini, 1976; Veggiani, 1974);
- hydrogeology (Carcano and Piccin, 2002; Baraldi and Zavatti, 1994; Baraldi and Pellegrini, 1976);
- geophysics (Pieri and Groppi, 1981; Cassano et al., 1986);
- historical documents (Calzolari, 1989; Marani, 1969 and 1966; Bevilacqua, 1734);

Previously it was supposed that the fluvial eastward diversion at Grazie could be related to an active fault south of the Mantova lake (Baraldi et al., 1980) named "Mantova Line" E-W striking, 15 km long and displacement unknown (Castaldini and Panizza, 1991). Following Serva (1990) it is a reactivation of an E-W buried fault.
Latest hypothesis related the River Mincio eastward deflection to an E-W trending blind thrust: high-angle, south dipping blind reverse fault according to De Martini et al. (1998); low angle, north dipping blind thrust according to Valensise and Pantosti (2001).

## *2.6. Remote sensing analysis*

Remote sensing analysis has been carried out on ASTER - EOS AM-1 Level-1B dataset. ASTER images have spatial resolution of 15 and 30 m and scenes of 60x60 km are provided. The River Mincio area is included in the scene 2001060702_118_001, free delivered by USGS EROS Data Center.
The image has been analysed using mainly the first six bands arranged in false color composition (e.g. 5:4:2, 4:2:1, 4:3:2; 3:2:1; 6:5:2; 3:3:1) and the single display of the first three bands, emphasised with common elaboration techniques (linear stretching, histogram equalize, gaussian, gamma, standard deviation). To avoid the influence of vegetation and emphasise lithology and moisture, ratio elaboration on bands 5, 4, 3 and 1 has been made (5/4, 4/3, 3/1) and the derived images have been analysed as before, but also using the "level slice" stretch (density slicing).
The main geomorphic units between Lake Garda and River Po are clearly discernible at full scene (Figure 5), from north to south they are:

- southernmost part of Lake Garda;
- morainic amphitheatre;
- River Mincio alluvial fan;
- River Chiese alluvial plain;
- River Mincio alluvial plain;
- Mantova Lakes;
- River Po.

In the middle of the study area, another kind of features has been noticed: it concerns two NW-SE elongated strips west and south of Mantova (Figure 5). On the satellite image, they can be seen well on 4:5:1 composition with "histogram equalize" stretching, the western one appears as a brighter belt, while the southern one is darker (118_9geo.bil 4:5:1, HE). These features cannot be easily ascribed to present-day landforms, geomorphological, lithological and soil units, as it results also from the comparison with the relevant maps, but there is some agreement with the hydrogeological units drawn by Baraldi and Pellegrini (1976).

### *2.6.1 Paleo-channels*

Several paleo-channels, concerning different river systems of various ages, have been identified (Figure 7). From west to east, the main paleo-channels have been assigned to the following river systems: Chiese, Osone, Mincio and Tione. In the southwestern sector between Chiese and Osone paleo-systems, a complex entrenchment of paleo-meanders is present, therefore the subsystem Fossaviva has been established.

The paleo-channel have been related to different time spans on the basis of:

- geomorphic characteristics (pattern, width, ...);
- degree of matching to the present-day surface (microrelief map and field survey);
- degree of visibility on the satellite image.

The oldest paleo-channels show a north-south direction, turning southeastward in the lower part, where they also seem to become more sinuous. They are supposed to be post-Middle Pleistocene in age based on the following remarks:

- higher concentration in the sector between Mincio and Chiese;
- clear visibility on the satellite image at full scene;
- great continuity and width;
- low sinuosity pattern;
- disappearance below the recent fans at the foot of the Garda morainic amphitheatre;
- weak or discontinuous matching with the present-day surface;
- presence of a partially outcropping moraines Middle Pleistocene in age (Carpenedolo and Sedena stages after Cremaschi, 1986).

These paleo-channels could represent the drainage evolution during the Middle Pleistocene-Late Pleistocene interglacial on the outwash plain built during the Carpenedolo and Sedena ice stages.
During the Late Pleistocene ice stage (Last Glacial Maximum; Solferino stage after Cremaschi, 1986) the meltwaters flowed mainly west of River Chiese and east of River Osone, so that the sector between these two rivers were undergone only to weak burial. Evidence of that is given by the arrangement/layout of the braided discontinuous small channels that built the LGM outwash plain (Figure 7).
The Early Holocene paleo-channels match better the present day-surface than the post-Middle Pleistocene ones. They display not always a great continuity, except the Fossaviva paleo-channel south of Grazie. Among Rivalta, Grazie and Buscoldo, there is a close net of Early Holocene paleo-meanders often broken off one another.
Starting from Early Holocene, during the retreat of the glacier, four major rivers (Chiese, Osone, Mincio and Tione) embedded their channels in the morainic amphitheatre, in the fans and in the outwash plain. Later in Holocene, Osone and Tione became minor channels and the only river today coming out from Lake Garda is the River Mincio. It has deepened and widened its valley shifting westwards between Goito and Mantova, eroding the western scarp and capturing the channels flowing from NW to SE.
The post-Early Holocene paleo-channels are narrow and discontinuous and they have been recognised only in the Mincio valley, particularly in its upper part.

### *2.6.2 Lineaments*

The remote sensing lineament detection has recognised five different trends: the most common is the E-W trend, followed by the N-S, the NNE-SSW, WNW-ESE and finally the NE-SW. These lineaments can be referred to different partly known fault systems (Castellarin and Cantelli, 2000; Picotti et al., 1995; Castellarin et al., 1987; 1992): the E-W trend could be related to the S-SE verging

south-alpine thrusts and folds and the NNE-SSW may be attributed to a southward prosecution of the Giudicarie fault system. The N-S trending and NE-S could be ascribed to the same system.
The lack of NW-SE trend could rule out the influence of the Schio-Vicenza fault system in the study area.
It is to be noticed that east of River Mincio only few lineaments have been recognised.
The lineaments detected on the satellite image have been compared to the lineaments highlighted by microrelief analysis (see chapter 7.2, Figure 10).

## *2.7. Microrelief analysis*

The microrelief map (contour interval 0.5 m) has been drawn out from the 1:10.000 technical maps of Regione Lombardia, by digitisation of the elevation points among morainic foothills River Chiese, River Po and Lombardia-Veneto boundary.
The most remarkable features on the microrelief map are the Mincio valley main scarps and the Fossaviva paleo-meanders.

In the area west of western Mincio main scarp, the N-S drainage trend is prevailing, while in the sector east of eastern Mincio main scarp, the drainage displays a NW-SE trend, but turning N-S in the lower part of this sector (Figure 8).
Several topographic profiles have been drawn using the same dataset; the most meaningful are shown in Figure 9.

The microrelief analysis has led to the result that there is no surface deformation due to a buried anticline between Grazie and Mantova. Anyway, some anomalous features have been highlighted and some of them match with the lineaments outlined by remote sensing analysis. Moreover, the microrelief analysis pointed out as the Fossaviva paleo-channel should not be related to a paleo-Mincio course cut off by diversion (see chapter 4.3 or 5).

### *2.7.1 Paleo-channels*

The clearest paleo-channel is the N-S meandering one named Fossaviva (south of Rivalta - Grazie), having a linear length of about 12 km. The microrelief analysis put in evidence as the Fossaviva paleo-channel should be related previously to the N-S paleo-channel just beside the western Mincio main scarp and successively to the Osone paleo-channels (Figure 8).
Only the most recent or the most entrenched paleo-channels can be identified on the microrelief map.

### *2.7.2 Lineaments*

Four groups of straight features have been recognised on the microrelief map: the N-S lineaments are prevailing, followed by the E-W trend and then by the NE-SW and the NNE-SSW trends. It must be pointed out the lack of lineaments east of eastern Mincio main scarp, whilst in the area between Chiese and Mincio rivers they can be easily singled out (Figure 10). The outcomes of remote sensing lineament analysis and microrelief lineament analysis are in good agreement, bearing in mind the different scale at which the two analyses have been conducted.

## *2.8. Discussion and conclusions*

The outcome of this research does not bear out the hypothesis of a surface deformation due to a growing buried anticline southwest of Mantova as well as any other suppose tectonic structure/line along the Grazie-Mantova scarp. Moreover, Agip-Eni unpublished seismic profiles do not show any buried anticline in this area. That is in spite of some anomalies present in the Mantova area (see chapter 5), first of all the sharp eastwards deflection of River Mincio.

The present research allows us to suggest an alternative hypothesis to explain the River Mincio fluvial "anomaly". It can be the consequence of the only geomorphological evolution of the area since Early Pleistocene. It must be pointed out as the present day location of the Mantova lake is not original. The pristine site was downstream Mantova (see chapter 4.3 and Figure 4). Otherwise, the eastward deflection at Grazie is quite natural, even if it seems as due to a River Mincio diversion and simultaneous entrenchment. The Mincio valley evolution looks like deeply influenced by pro- and periglacial processes.

A periglacial drainage system was driven by the ice-marginal depressions developed during the older ice ages (Early-Middle Pleistocene). Based on water-wells stratigraphy in Mantova surroundings and the erratic boulders (Figure 7) found at Bigarello Redondesco, Casatico (about 20 km west of Mantova; Gozzi, 1973) and Gazzo Veronese (about 20 km east of Mantova; Sorbini et al., 1984), the new hypothesis, supposes that an older glaciation extended its ice front very close to Mantova.

The analysis of the water-wells stratigraphy highlighted the presence of clay layers thicker than 10 meters north of Mantova, where gravel and sand are prevailing. In such an environment, a fluvial origin is unlikely, instead their relationship with morainic lakes is more probable. To support the supposed presence of buried glacial deposits, in some water-wells stratigraphy layers of mixed sand, gravel and clay or gravel and clay are reported (Figure 7). This kind of unsorted lithology, in fact, is peculiar of tills.

It could be hypothesised that a glacier reached the Mantova latitude and the Mincio valley downstream this point represent a "sandur valley" related to a meltwater channel. It is also supposed that a W-E ice marginal depression west of Mantova could exist during that ice stage in analogy with the model of an ice front decoupled from its sandur (Magillian et al., 2002; Evans and Twigg, 2002; Gomez et al., 2000; figure 11). These ice proximal landforms were preserved, as the subsequent glaciers did not reach this area, so that later those ice marginal depressions and sandur valleys influenced the drainage evolution.

Here it is supposed that after the LGM the paleo-Mincio flowed close to its eastern scarp and minor channels run toward and along the Mantova depression (Figure 7). Not far east the Tione was another main meltwater channel, but later this melt-channel was abandoned, more water flowed into the melt-channel Mincio and greater entrenchment of the riverbed took place. It can be supposed that the water discharge was moreover increased when the ground-water table was intercepted by the river-bed deepening, so enhancing the erosion especially at the foot of the morainic arc.

At a certain time, between Pozzolo and Goito the Mincio diverted its course and shifted westwards eroding the western scarp and capturing the minor channels, which were flowing from NW to SE toward the Mantova depression. Finally, between Rivalta and Grazie the River Mincio cut the eastern meanders of the Fossaviva river system, let the western ones hanging on the Mincio valley.

Concluding, this research has brought forward the following results:

- there is no evidence of surface deformation due to a buried growing anticline;
- the sharp deflection of River Mincio at Grazie is not to relate to any tectonic buried or exposed structure; on the contrary it appears as the result of fluvial dynamics and drainage evolution driven by inherited proglacial/periglacial landforms;
- according to Baraldi and Pellegrini (1976) the Fossaviva paleo-channel is not the paleo-Mincio, but represents the southern part of a different paleo-channel.

## *2.9. References*

Arca S. and Beretta G.P. (1985) – Prima sintesi geodetico-geologica sui movimenti verticali del suolo nell'Italia Settentrionale (1897-1957). Boll. Geod. Sc. Affini, 44, 125-156.

Baraldi F. and Pellegrini M. (1976) – Falde acquifere della Provincia di Mantova. C.N.R. P/335, Quaderni Istituto Ricerca sulle Acque, 28 (6), 183-208.

Baraldi F. and Zavatti A. (Eds) (1994) – Studi sulla vulnerabilità degli acquiferi – Provincia di Mantova. Quad. di tecniche di protezione amb. n. 34, vol. 5, 120 pp., pubbl. GNDCI-CNR N. 889.

Baraldi F., Carton A., Castaldini D., Panizza M., Pellegrini M. and Sorbini L. (1980). Neotettonica di parte dei fogli Peschiera del Garda (48), Verona (49), Mantova (62) e di tutto il foglio Legnago (63). C.N.R., Prog. Fin. Geodinamica, Contrib. Realizz. Carta Neotettonica d'Italia, Publ. 356, Giannini, Napoli, 643-655.

Bevilacqua E. (1734) – Informazione sopra gli argini, sgoli, ed adacquamenti dello Stato Mantovano. Stamperia di San Benedetto, Mantova.

Bini A., Cita M.B., and Gaetani M. (1978). Southern Alpine lakes – Hypothesis of an erosional origin related to the Messinian entrenchment. Mar. Geol., 27, 289-302.

Burrato P., Ciucci F. and Valensise G. (1999). Un approccio geomorfologico per la prima individuazione di strutture potenzialmente sismogenetiche nella Pianura Padana. Proc. XVIII meeting GNGTS, Rome 9-11 November 1999.

C.N.R. (1983). Neotectonic Map of Italy. Prog. Fin. Geodinamica, 114. Quad. Ric. Scient., 4; 6 fogli, scala 1:500.000, SELCA, Firenze.

Calzolari M. (1989). Padania romana – Ricerche archeologiche e paleoambientali nella pianura tra il Mincio e il Tartaro.

Carcano C. and Piccin A. (2002). Geologia degli acquiferi padani della Regione Lombardia. Regione Lombardia – Eni Divisione Agip, Selca Firenze 2002, 130 pp, 10 tav.

Cassano E., Anelli L., Fichera R. and Cappelli V. (1986). Pianura Padana. Interpretazione integrata di dati geofisici e geologici. Agip, 73° Congresso Società Geologica Italiana, Roma 29 sett. 4 ott. 1986, 27 pg.

Castaldini D. and Panizza M. (1988). Contributo alla definizione del limite tra evidenze di neotettonica e fenomeni dovuti ad altre cause. Geogr. Fis. Din. Quat., Suppl. 1, 11-23.

Castaldini D. and Panizza M. (1991). Inventario delle faglie attive tra i fiumi Po e Piave e il Lago di Como (Italia Settentrionale). Il Quaternario, 4, 333-410.

Castaldini D. (1989). Evoluzione della rete idrografica centropadana in epoca protostorica e storica. Atti Convegno Naz. Studi "Insediamenti e Viabilità nell'alto Ferrarese dall'età romana al Medioevo", Cento, maggio 1987, Acc. Sc. di Ferrara, 115-134.

Castellarin A. and Cantelli L. (2000). Neo-Alpine evolution of the Southern Eastern Alps. J. of Geodynamics, 30, 251-274.

Castellarin A. and Vai G.B. (1986). Southalpine versus Po Plain Apenninic Arcs. In: The origin of the Arcs (F.C. Wenzel ed.), Development in Geotectonics, 21, Elsevier, Amsterdam, 253-280.

Castellarin A. (1994). L'architettura geologica. In: Gorfer A. and Turri E. (eds.) "Là dove nasce il Garda", Verona 1994, 15-34.

Castellarin A., Cantelli L., Fesce A.M., Mercier J.L., Picotti V., Pini G.A., Prosser G., Selli L. (1992). Alpine compressional tectonics in the Southern Alps. Relationships with the N-Apennines. Annales Tectonicæ, VI, n.1, 62-94.

Castellarin A., Fesce A.M., Picotti V., Pini G.A., Sartori R.,Selli L., Cantelli L., Ricci R. (1986/87). Structural and kinematics analysis of the Giudicarie deformation belt. Implications for coimpressional tectonics of Southern Alps. Miner. Petrogr. Acta, 30, 286-310.

Castellarin, A., Sartori, R. (1983). Il sistema tettonico delle Giudicarie, della Val Trompia e del sottosuolo dell'Alta Pianura Lombarda. Mem. Soc. Geol. It., 26, 31-37.

Castiglioni G. B. And Pellegrini G.B. (EDS) (2001). Note illustrative della carta geomorfologica della Pianura Padana. Suppl. di Geografia Fisica e Dinamica Quaternaria, IV – 2001.

Castiglioni G.B., Ajassa R., Baroni C., Biancotti A., Bondesan A., Bondesan M., Brancucci G., Castaldini D., Castellaccio E., Cavallin A., Cortemiglia F., Cortemiglia G.C., Cremaschi M., Da Rold O., Elmi C., Favero V., Ferri R., Gandini F., Gasperi G., Giorgi G., Marchetti G., Marchetti M., Marocco R., Meneghel M., Motta M., Nesci O., Orombelli G., Paronuzzi P., Pellegrini G.B., Pellegrini L., Rigoni A., Sommaruga M., Sorbini L., Tellini C., Turrini M.C., Vaia F., Vercesi P.L., Zecchi R. and Zorzin R. (1997). Carta Geomorfologica della Pianura Padana a scala 1:250.000. Selca, Firenze.

Cremaschi M. (1987). Paleosols and Vetusols in the Central Po Plain (Northern Italy): a study in Quaternary Geology and soil development. Centro Grafico Linate (MI), 306 pp.

De Martini P., Burrato P. and Valensise G. (1998). Active tectonic structures in the Padana Plain: new discrimination strategy from a joint study of geomorphic and geodetic levelling data. In: Proceedings of the EGS Annual Meeting, Nice, France, April 1998.

Doglioni C. (1993). Some remarks on the origin of foredeeps. Tectonophysics, 228, 1-20.

Evans D.J.A. and Twigg D.R.. The active temperate glacial landsystem: a model based on Brei_amerkurjökull and Fjallsjökull, Iceland. Quaternary Science Reviews, 21 (20-22), 2143-2177.

Finckh P.G. (1978). Are southern Alpine Lakes former Messinian canyons?- Geophysical evidence for preglacial erosion in the southern Alpine lakes. Mar. Geol., 27, 289-302.

Gomez B., Smith L.C., Magilligan F.J., Mertes L.A.K. and Smith N.D. (2000) . Glacier outburst floods and outwash plain development: Skei_aràrsandur, Iceland. Terranova, 12, 126-131, 2000.

Gozzi G. (1973). Il territorio mantovano – Studio di geologia. Civiltà Mantovana, VII; quad. 38, 69-119.

Magilligan F.J., Gomez B., Mertes L.A.K., Smith L.C., Smith N.D., Finnegan D. and Garvin J.B. (2002). Geomorphic effectiveness, sandur development, and the pattern of landscape response during jökulhlaups: Skei_aràrsandur, southeastern Iceland. Geomorphology, 44, 95–113.

Marani E. (1967). Il paesaggio lacustre di Mantova fra l'antichità romana e il Medio Evo. Parte prima. Civiltà Mantovana n. 8, 93-114.

Marani E. (1967). Il paesaggio lacustre di Mantova fra l'antichità romana e il Medio Evo. Parte seconda. Civiltà Mantovana n. 11, 361-387.

Marani E. (1969). Indicazioni documentarie fondamentali sulle tre cerchie di Mantova. Civiltà Mantovana n. 22, 225-240.

Marchetti M. (2002). Environmental changes in the central Po Plain (northern Italy) due to fluvial modifications and anthropogenic activities.Geomorphology, 44 (2002) 361–373.

Nicolis E. (1898). Sugli antichi corsi del fiume Adige. Contribuzione alla conoscenza della costituzione della pianura Veneta. Boll. Soc. Geol. It. XVII, 6-75.

Ogniben L. (1986). Modello geodinamico della regione trentina e aree circostanti. Studi trent. Sci. nat., Acta geol., 63/1986, 1-165.

Picotti V., Prosser G. and Castellarin A. (1995). Structures and kinematics of the Giudicarie. Val Trompia fold and thrust belt (Central Southern Alps, Northern Italy). Mem. Sc. Geol., 47, 95-109.

Pieri M. and Groppi G. (1981). Subsurface geological structure of the Po Plain, Italy. C.N.R., Prog. Fin. Geodinamica, Sottoprog. Modello Strutturale, Pubbl. 414, 1-30.

Serva L. (1990). Il ruolo delle Scienze della Terra nelle analisi di sicurezza di un sito per alcune tipologie di impianti industriali: il terremoto di riferimento per il sito di Viadana (MN). Boll. Soc. Geol. It., 109, 375-411.

Sleiko D., Carulli G.B., Carraro F., Castaldini D., Cavallin A., Doglioni C., Iliceto V., Nicolich R., Rebez A., Semenza E., Zanferrari A. and Zanolla C. (1987). Modello sismotettonico dell'Italia nord- orientale, C.N.R. – Gr. Naz. Dif. Terremoti, Rendiconto 1, Trieste, 82 pp.

Sorbini L., Accorsi C.A., Badini Mazzanti M., Forlani L., Gandini F., Meneghel M., Rigoni A. and Sommaruga M. (1984). Geologia e geomorfologia di una porzione della pianura a sud-est di Verona. Mem. Mus. Civ. St. Nat. Verona, sr. 2, sez Sc. Terra, 2, 92 pp.

Valensise G. and Pantosti D. (Eds.) (2001). Databaseof potential sources of earthquakes larger than M 5.5 in Italy. Annali di Geofisica, Suppl. to vol 44(4), 180 pp., with CD-ROM, 2001.

Veggiani A. (1974). Le variazioni idrografiche del basso corso del Po negli ultimi 3000 anni. Padusa 1-2, 22 pp.

Venzo S. (1957). Rilevamento geologico dell'anfiteatro morenico del Garda, parte I, tratto occidentale Gardone-Desenzano. Mem. Soc. It. Sci. Nat., vol2 (2), 73-140.

Zanferrari A., Bollettinari G., Carobene L., Carton A., Carulli G.B., Castaldini D., Cavallin A., Panizza M., Pellegrini G.B., Pianetti F. and Sauro U. (1982). Evoluzione neotettonica dell'Italia nord-occidentale. Mem. Sc. Geol., Univ. Padova, 35, 355-376.

**Figure 1.** Geomorphological units of central Po Plain (after Marchetti, 2002). Keys: (1) Holocene fluvial deposits unit, (2) Late Pleistocene bajada unit, (3) Po Plain unit, (4) old terraces unit, (5) moraines, (6)

**Figure 2.** Structural sketch of Lake Garda area (after Castellarin, 1994).

**Figure 3.** Geomorphological map of River Mincio area (after Castiglioni et al., 1997).

**Figure 4.** Mantova Lake supposed extent (in black) before hydraulic schemes of XII century (after Marani, 1967a).

**Figure 5.** Aster image of the study area: scene 2001060702_118_001, free delivered by USGS EROS Data Center.

**Figure 6.** Aster image of the study area: scene 2001060702_118_001, free delivered by USGS EROS Data Center.

**Figure 7.** Remote sensing geomorphological interpretation.

**Figure 8.** Microrelief drainage analysis.

**Figure 9.** Selected profiles across the "Mantova anticline" and nicrorelief map of the middle reach of River Mincio, showing profiles trend and location. Contour interval is 0.5 m.

**Figure 10.** Comparison between remote sensing lineament analysis and microrelief lineament analysis.

**Figure 11.** Model for the W-E scarp between Mantova and Grazie (after Gomez et al., 2000).

# Section 3 – The Mirandola – Secchia and Panaro rivers area (southern-central Po Plain)

**by Pierfrancesco Burrato, Francesca Ciucci and Gianluca Valensise**

## *3.1. Introduction*

The Mirandola Source is a blind, N-verging thrust located at the western termination of the buried Ferrara Arc. It is associated with a well-expressed buried anticline and controls the recent drainage pattern evolution as it is shown by numerous river diversions. No historical and instrumental seismicity can be associated with this major buried structure. The location of the Mirandola Source was determined using subsurface geological and geophysical data, constrained by analitical modeling of drainage anomalies. The expected vertical deformation induced by various fault models have been compared a) in map view with the mean drainage directions and the locus of drainage attraction and diversion, and b) in 2D cross-sections with the geometry of sintectonic growth-strata. The best fitting fault model have been chosen as the causative source of the obeserved geomorphic anomalies and of the geologic deformation.

Based on the analysis of the subsurface data provided by the oil industry (Cassano et al., 1986; Pieri and Groppi, 1981; Regione Emilia Romagna and ENI-Agip, 1998) and on geomorphological observations provided by several investigators (e.g. Castaldini et al., 1979; Veggiani, 1985), we propose that the Mirandola Source is a major blind thrust having the following geometrical characteristics:

- *length*: 18.0 km; the length is based on scaling with width and constrained by geomorphological observations and dislocation modeling.
- *width*: 14.0 km; the down-dip width is based on the characteristic distance between the synclinal and anticlinal axes and on the assumptions made concerning the minimum and maximum faulting depth; the syncline and anticline position has been constrained by gemorphic and geologic observations;
- *strike*: N100°; the NW-SE strike is chosen according with the general orientation of the buried tectonic structures;
- *dip*: 25°; the fault dip is towards the S, in agreement with subsurface evidence and based on the general direction of dip of the thrust faults of the buried Northern Apennines fronts;
- *rake*: 90°; the rake is assumed to be that of a pure thrust movement, and is based on the strike of the fault and on general geodynamic considerations concerning the regional direction of compression;
- *depth*: 6.0-12.0 km; the minimum and maximum depth are constrained by subsurface geology, by the symmetry of the anticline and by the general aspect-ratio of the anticline-syncline couple.

## 3.2. Previous investigations

Only few specific studies exist on the Mirandola Source. Nevertheless, information on the location, geometry and recent activity of the source can be obtained from a number of papers dealing with the subsurface geology and geomorphology of the Po Plain.

Castaldini et al. (1979) in the framework of a reconstruction of the neotectonic events of the Po Plain, examine the evolution of the drainage system of this part of the Po Plain. The analysis considers the full length of the Holocene but special emphasis is given to the past three thousand years of progressive shift and sudden diversions of the main streams of the area. In particular, the authors point out that the Secchia and Panaro rivers are first attracted towards each other and towards the axis of the so-called Bologna-Bomporto-Reggio Emilia syncline, then pushed sideways respectively towards the NW and E as they cross the alignment Carpi-Crevalcore. Castaldini et al. (1979) also describe important diversions that occurred after the VIII century B.C., particularly affecting the Po river that turned northward at Guastalla ("rotta di Guastalla"), the Secchia river turning east just north of Modena, and again the Secchia river turning northwest a few km South of Mirandola. Finally, they describe the occurrence of some surface faults 1) in the area Mirandola-Concordia, discovered on the basis of correlations of the stratigraphy of water wells, 2) in the area of Canalazzo di Finale Emilia, based on observations in the field of open ground cracks aligned along a WNW trend, and 3) near Correggio, based on observations of fractures in walls and road pavements. This last fault is also seen in satellite imagery.

Veggiani (1985) proposes a scheme for the evolution of the Secchia, Panaro, Crostolo and Reno rivers during the past 3,000 years in the context of a reconstruction of paleo-channels of the Po river and of its main tributaries. In particular, he proposes a dated sequence of progressive shifts of the Secchia and Panaro rivers up to their present position.

Cassano et al. (1986) provide a comprehensive summary of subsurface and surface data along several transects crossing the Po Plain from the Southwest to the Northeast. Their interpretation of Section 9 shows a major anticline driven by a low-angle north-verging blind thrust culminating between Mirandola and Medolla.

Burrato et al. (1999, 2003) analyse in detail the fluvial system of the Po Plain and identify several areas where significant drainage anomalies (e.g., river diversions and shifts in channel patterns) with wavelength comparable to that of tectonic structures of crustal significance are suggestive of the presence of active blind thrust or reverse faults. As second step of their approach the authors to corroborate the hypothesis of the tectonic nature of the anomalies compare their position with the location of known buried anticlines. Following the observation that some of the anomalies are associated also with historical earthquakes, they propose that these blind thrusts may be potential sources of rather infrequent large earthquakes beneath the Po Plain. Burrato and coworkers also show that the Secchio and Panaro rivers exhibit significant anomalies in their trend as they cross an anticline reported in the official geological map. They interpret the fluvial anomaly as having tectonic origin.

Ciucci et al. (2002) study the Mirandola Source using an approach that combines geomorphic and subsurface geologic observations. They show that in the subsurface the deformation is expressed by a mature anticline and involves the entire sedimentary suite up to the surface. Besides they use the contoured subsurface structural horizons to relate the observed anomalies and deformation to sustained slip on a north-verging, large blind thrust fault located beneath Mirandola. The authors constrain to 1.7 mm/y the slip rate of the fault modelling in 2D the growth strata. They also point out that similarly to other faults along the northern Apennines margin, this fault could be seismogenic and produce a M≤6.2 earthquake. A different scenario would involve aseismic or episodically seismic slip along the entire fault plane or portions of it.

## 3.3. Expected seismic behaviour

Current catalogues (CPTI Working Group, 1999, CFTI, 1997) report no historical earthquakes located in the area around the source. The only earthquake that falls close to the Mirandola blind thrust (22 February 1346, Me 6.8 Ferrara earthquake) seems to be mislocated and overrated having only three intensity data point scattered in a wide region. The recent activity of the buried thrust front is shown by the 1996 Mw 5.4 Reggio Emilia earthquake located on the lateral transpressional ramp of the Ferrara Arc to the WSW of the Mirandola Source.

Based on analysis of sintectonic growth strata dated to 0.4 My (Ciucci et al., 2002; Regione Emilia Romagna and ENI-Agip, 1998) the slip rate of the Mirandola Source has been constrained to about 1.7 mm/y. This value may be an upper bound since it has been calculated without correcting the differential compaction that could have enhanced the topographic contrast between the anticline and syncline axes.

The seismic and kinematic parameters associated to the Mirandola Source are the following:

- *last earthquake*: unknown;
- *previous earthquakes*: unknown;
- *recurrence interval*: 600 years; inferred from slip rate and average displacement; a minimum recurrence interval of 700 years is constrained by historical evidence;
- *elapsed time*: unknown;
- *slip rate*: 1.7 mm/y from analysis of growth strata;
- *average displacement*: 1.0 m; calculated from Mo;
- *expected magnitude*: 6.5 (Mw) from geological data.

## 3.4. Discussion and conclusions

This source belongs to the outermost propagation of the Apennines compressional wedge and is well expressed in the subsurface with a mature anticline. The study of the paleo-depocenters showed that they migrated consistently towards the north-west up to the present one indicated by the area where the Secchia and Panaro rivers are attracted, suggesting that the drainage anomaly is due to the ongoing tectonic subsidence.

According to Castaldini et al. (1979), after the VIII century B.C. the Po and Secchia rivers suffered major diversions that are in agreement with the expected pattern of vertical deformation associated with repeated motion on the underlying fault.

Given the estimated width and length, the fault is capable of generating a M 6+ earthquake that would have its strongest effects in a broad region between the Po river and the Apennines piedmont. Current catalogues (CPTI Working Group, 1999) report a large event in 1346 (Me 6.8) that falls very close to the Mirandola Source. However, both the location and the magnitude of this event are highly uncertain due to the very limited number of data available.

The Mirandola, Concordia and Canalazzo di Finale Emilia surface faults described by Castaldini et al. (1979) follow the trend of the anticline and fall on its northern flank near the hinge of the fold. These faults could be interpreted as extensional features associated with bending at the top of the rising structure.

In spite of the limited geomorphic expression, the Mirandola Source is very well developed in the subsurface. The frequent and substantial diversions and shifts of the rivers flowing around it suggest that this is a rather fast structure. Substantial tectonic rates are also suggested by the observation that the tectonic signal is enough to compensate the accumulation of sediments by the Secchia and Panaro rivers.

The 1.7 mm/y slip rate calculated by Ciucci et al. (2002) is in agreement with the geomorphic observations that imply a fast growing buried anticline. However it is in contrast with the absence of historical and instrumental seismicity, since with such a fast slip rate the fault should generate earthquakes with a recurrence interval shorter than the interval of completeness of the catalogues.

The slip rate was calculated using the topographic contrast between the anticline and syncline axes of the 0.4 My structural horizon. The value obtained could be an upper bound, since it may have been enhanced by differential compaction phenomena. The calculation of the slip rate made using the 0.65 My horizon yielded a comparable value of 1.6 mm/y, while the same calculation made using a 3.6 My horizon returned 0.4 mm/y. This observation indicate that the time of inception of the fault is between the two lower horizon, perhaps closer to the upper one.

The identification and characterization of a major active fault beneath Mirandola raises fundamental questions concerning the seismogenic potential of this source. The first question concerns whether the slip rate calculated by Ciucci et al. (2002) is truly representative of tectonic activity. Further work is needed to assess how much this estimate is affected by differential compaction phenomena. A second and even more important question concerns the expected seismogenic behavior of the Mirandola fault. Will it rupture in large M 6+ rather infrequent events? Or in smaller more frequent earthquakes in the M range 5-5.5? Or is it totally aseismic? This fundamental question could be addressed by carefully analyzing the evolution of this structure and particularly its modern strain pattern using conventional geodetic data or SAR interferometry. Such observations would allow any locked (i.e., seismogenic) portions of the fault plane to be correctly identified and characterized.

## 3.5. References

Argnani, A., G. Barbacini, M. Bernini, F. Camurri, M. Ghielmi, G. Papani, F. Rizzini, S. Rogledi and L. Torelli (2003). Gravity tectonics driven by Quaternary uplift in the Northern Apennines: insights from the La Spezia-Reggio Emilia geo-transect. *Quatern. Int., 101-102, 13-26.*

Barozzi, P., and L. Colombi (1992). Profilo CROP-01/01A, sezioni sismiche e geologiche e ipotesi di tracciato del profilo nella Pianura Padana. in: R. Capozzi and A. Castellarin (eds), Studi preliminari all'acquisizione dati del profilo CROP 1-1A La Spezia-Alpi Orientali. Studi Geologici Camerti, spec. vol. 1992/2, 161-170.

Bonori, O., M. Ciabatti, S. Cremonini, R. Di Giovambattista, G. Martinelli, S. Maurizzi, G. Quadri, E. Rabbi, P. V. Righi, S. Tinti and E. Zantedeschi (2000). Geochimical and geophysical monitoring in tectonically active areas of the Po Valley (Northern Italy). Case histories linked to gas emission structures. *Geogr. Fis. Din. Quat., 23, 3-20.*

Burrato, P., F. Ciucci and G. Valensise (1999). Un approccio geomorfologico per la prima individuazione di strutture potenzialmente sismogenetiche nella Pianura Padana. Proc. 18° Meeting G.N.G.T.S., Roma November 9-11, 1999, 19 p.p..

Burrato, P., F. Ciucci and G. Valensise (2002). Is the Po Plain a low seismic hazard region? Proc. ESC General Assembly, Genova 1-6 September 2002.

Burrato, P., F. Ciucci and G. Valensise (2003). River response to blind thrust faulting in the Po Plain, northern Italy. in press on *Ann. Geophys.-Italy*.

Cassano, E., L. Anelli, R. Fichera and V. Cappelli (1986). Pianura Padana. Interpretazione integrata di dati geofisici e geologici. Proc. 73° Meeting Società Geologica Italiana, September 29. October 4 1986, Roma Italia, pp. 27.

Castaldini, D., G. Gasperi, M. Panizza and M. Pellegrini (1979). Neotettonica dei Fogli 74 (Reggio nell'Emilia) (p.p.) e 75 (Mirandola) nell'intervallo da 18.000 B.P. all'Attuale (interv. V). C.N.R., Nuovi contributi alla realizzazione della Carta Neotettonica di Italia, publ. n. 251 of Progetto Finalizzato Geodinamica, 317-332.

Castellarin, A., C. Eva, G. Giglia, G. B. Vai, E. Rabbi, G. A., Pini and G. Crestana (1985). Analisi strutturale del Fronte Appenninico Padano. *Giorn. Geol., s. 3a, 47/1-2.*

Ciaccio, M.G., and C. Chiarabba (2003). Tomographic models and seismotectonics of the Reggio Emilia region, Italy. *Tectonophysics, 344, 261-276*.

Ciucci, F., P. Burrato and G. Valensise (2002). Complex geomorphic response to blind thrust faulting along the northern margin of the Apennines near Mirandola (Po Plain). Proc. ESC General Assembly, Genova 1-6 September 2002.

Ciucci, F., P. Burrato and G. Valensise (2002). Deformazione attiva dovuta a thrust ciechi lungo il margine settentrionale appenninico: l'esempio dell'anticlinale di Mirandola (Modena). Proc. 21° Meeting G.N.G.T.S., Rome 2002.

Cremaschi, M., and A. Marchesini (1978). L'evoluzione di un tratto di Pianura Padana (Prov. Reggio e Parma) in rapporto agli insediamenti ed alla struttura geologica tra il XV sec. a.C. ed il sec. XI d.C.. Archeologia Medioevale, V, Edizioni CLUSF.

Cremaschi, M., and G. Gasperi (1989). L'alluvione alto-medioevale di Mutina (Modena) in rapporto alle variazioni ambientali oloceniche. *Mem. Soc. Geol. It., 42, 179-190.*

Fazzini, P., G. Gasperi and R. Gelmini (1976). Litologia di superficie dell'alta e media pianura modenese. *Proc. Soc. Nat. e Mat. di Modena, 107.*

Gasperi, G., and M. Pellegrini (1969). Le falde acquifere della pianura compresa tra Secchia, Panaro e Po. Proc. 1° Conv. Naz. Studi sui Probl. di Geol. Appl., VI, SA.MO.TER.

Gasperi, G., and M. Pellegrini (1968). Movimenti tettonici recenti nella zona di Mirandola (Pianura modenese). *Proc. Soc. Nat. e Mat. di Modena, 99.*

Istituto di Geologia dell'Università di Modena (1978). Metodologie e primi risultati di neotettonica nel Modenese e territori limitrofi. *Mem. Soc. Geol. It., 19, 551-562.*

Lavecchia G., P. Boncio, and N. Creati (2003). A lithospheric-scale seismogenic thrust in central Italy. *J. Geodynamics, 36, 79-94.*

Montone, P., and M. T. Mariucci (1999). Active stress along the NE external margin of the Apennines: the Ferrara arc, northern Italy. *J. Geodynamics, 28, 251-265.*

MURST-Ministry of University and Scientific and Technological Research (1997). Geomorphological map of relief and vertical movements of Po Plain, scale 1:250.000. Published by S.El.Ca., Florence, 3 sheets.

MURST-Ministry of University and Scientific and Technological Research (1997). Geomorphological map of Po Plain, scale 1:250.000. Published by S.El.Ca., Florence, 3 sheets.

Panizza, M. (1975). Neotectonic and lithological implication in the course of the Secchia and Panaro Rivers (Northern Italy). *Studia Geomorph. Carpatho -Balcanica, 9, 6 pp.*

Panizza, M., D. Castaldini, G. Bollettinari, A. Carton and F. Mantovani (1987). Neotectonic research in applied geomorphological studies. *Z. Geomorph. N. F., Suppl. Bd 63: 173-211.*

Pellegrini, M. (1969). La pianura del Secchia e del Panaro. *Proc. Soc. Nat. e Mat. di Modena, 100.*

Pellegrini, M., A. Colombetti and A. Zavatti (1976). Idrogeologia profonda della pianura modenese. *Quad. Ist. Ric. sulle Acque, 28 (7).*

Pellegrini, M., and L. Vezzani (1978). Faglie attive di superficie nella Pianura Padana presso Correggio (Reggio Emilia) e Massa Finalese (Modena). *Geogr. Fis. Din. Quat., 1, 141-149.*

Pellegrini, M., F. Gemelli, E. Giliberti Neviani and A. Ragni (1977). Le acque sotterranee ad elevato contenuto alogenico della bassa pianura modenese-mantovana (Pianura Padana). *Quad. Ist. Ric. sulle Acque, 34 (1).*

Pieri, M., and G. Groppi (1981). Subsurface geological structure of the Po Plain (Italy). C.N.R., publ. n. 414 of Progetto Finalizzato Geodinamica, 23 pp..

Regione Emilia Romagna, ENI-Agip (1998). Riserve idriche sotterranee della Regione Emilia-Romagna. Di Dio G. (ed), Technical report and 9 maps, S.EL.CA. (Firenze), 120 pp..

Selvaggi, G., F. Ferulano, M. Di bona, A. Frepoli, R. Azzara, A. Basili, C. Chiarabba, M. G. Ciaccio, F. Di luccio, F. P. Lucente, L. Margheriti and C. Nostro (2001). The Mw 5.4 Reggio Emilia 1996 earthquake: active compressional tectonics in the Po Plain, Italy. *Geophys. J. Int., 144, 1-13.*

Veggiani, A. (1985). Il delta del Po e l'evoluzione della rete idrografica padana in epoca storica. Atti della Tavola Rotonda tenuta a Bologna il 24/11/1982 su "Il delta del Po, Sezione geologica", 37-68, Bologna 1985.

Veggiani, A. (1974). Le variazioni idrografiche del basso corso del Fiume Po negli ultimi 3.000 anni. *Padusa 1-2, 22 pp..*

**Figure 1**. Distribution of drainage anomalies in the Po Plain (marked in yellow). Their location was compared with that of the buried anticlinal axes (marked in red), and with historical seismicity (CPTI Working Group, 1999). Dashed black circles labelled A outline areas where a good correlation among these three elements exists. Dashed black circles labelled B indicate correlation of surface and subsurface data but no evidence for historical seismicity. Finally, the dashed red circles highlight three anomalies that for their importance require further investigations (from Burrato et al., (2003)). The Mirandola Source is located in the central part of the southern Po Plain at the western end of the Ferrara folds. This prominent buried anticline has not been associated with any historical earthquake, but controls the drainage pattern evolution forcing the Secchia and Panaro rivers to divert around the uplifting anticlinal crest (anomalies # 24 and 26) (from Burrato et al. (2003)).

**Figure 2**. Subsurface geological section from oil industry data. The Mirandola Source is aligned with the outermost anticlines of the Apennines thrust belt. South of the anticline all Quaternary deposits are warped into a gentle syncline (from Cassano et al. (1986)).

**Figure 3**. Following the interpretation of the subsurface geology given by an Agip cross-section, the Mirandola Source is interpreted to be a blind thrust confined between 3 and 8 km of depth and dipping 30° southward (from Cassano et al. (1986), modified).

**Figure 4**. Recent evolution of Panaro and Secchia rivers. South of Mirandola Source both rivers are attracted towards the syncline; more to the North the Secchia R. is progressively shifted northwestward by the growing anticline (from Castaldini et al. (1979)).

**Figure 5**. Recent evolution of the Po R. and main tributaries. The Mirandola Source is responsible for the attraction of the Panaro and Secchia rivers towards the syncline North of Modena, while the Po R. seems to be shifted northward (from Veggiani (1985)).

**Figure 6**. Fresh water-salt water interface in the Mirandola area, illustrating the spatial relationships between the anticline (to the NE) and the syncline (to the SW) (from Castaldini et al. (1979)).

**Figure 7**. Surface ruptures mapped by stratigraphic correlation of water wells and field surveys. They locate close to the hinge of the growing anticline and can therefore be interpreted as secondary extrados features (from Castaldini et al. (1979)).

**Figure 8**. Cross-section across the Mirandola anticline, showing extrados normal faulting dropping its northeastern limb and culmination of the marine deposits (from Panizza and Castaldini (1987)).

**Figure 9**. Summary of inferred vertical movements during the Holocene in the southern side of the Po River alluvial plain. The vertical movements and their sign have been inferred from the drainage evolution (from Panizza and Castaldini (1987)).

**Figure 10**. Cross-section drawn to calculate the slip rate of the Mirandola Source. The method compares the topographic contrast between anticline and syncline in the subsurface with the expected vertical displacement of the best fitting fault model. About 670 m of slip on a 25°-dipping thrust fault are necessary to reproduce the 260 m of topographic contrast of the 400 ky structural horizon (from Ciucci et al. (2002)).

**Figure 11**. Expected vertical displacement of the Mirandola Source compared with the drainage pattern evolution. The fault (shown in dark red) is a blind, N-verging thrust that induces uplift of a wide area. The Secchia and Panaro rivers are first attracted towards the syncline, then downstream of it cross the anticline, which uplift force the Secchia R. to shift its course northwestward. To the north the Po River follows a wide concavity that mimicks the contour of the uplifting area. (from Ciucci et al. (2002)).

# Section 4 – The Soncino. Oglio River area (western Po Plain)

**by Pierfrancesco Burrato and Gianluca Valensise**

## *4.1. Introduction*

Alluvial plains are among the most densely populated areas worldwide. This is the result of a combination of morphological, hydrological and geological factors that make them advantageous for human settlements. However, often they are located in active regions, and their flat surface resulting from a high sediment supply from nearby high relief areas may hide blind faults posing a significant seismic hazard. A striking example is the Los Angeles basin in California, located at the transform Pacific margin of the North American plate (Wright, 1991). Here more than 12 million people live in an area prone to destructive though moderate earthquakes generated by blind or elusive thrusts (e.g.: Hauksson *et al.*, 1988; Dolan *et al.*, 1995; Shaw and Suppe, 1996). Given the hidden nature of these seismogenic faults and related structures, they have been traditionally explored only by means of indirect methods such as interpretation of growth strata (e.g.: Suppe *et al.*, 1992), geodesy (e.g.: Lin and Stein, 1989; Massonet et al., 1993) and morphotectonic studies (e.g.: Bullard and Lettis, 1993).

The aim of this work is to present a geomorphological method for the identification of blind active faults associated with subdued topographic expression. We focused on the Po Plain, a low-relief sedimentary basin intensely deformed by buried folds and thrusts, as revealed by extensive oil exploration (Figure 1). In spite of the occurrence of historical earthquakes up to magnitude 6.5, the activity of individual tectonic structures is poorly known. The Po Plain is one of the most densely populated areas of Italy, has a rich patrimony of old historical towns, and represents the most important concentration of industrial facilities country-wide. In contrast with its high vulnerability, it is traditionally considered a region of low seismic hazard (e.g.: Albarello et al., 2000). Current historical catalogues list very few large earthquakes in the area and show that most of them do not exceed $M_e$ 5.5 (equivalent magnitude from CPTI Working Group, 1999). Most of the seismicity is concentrated south of the Po River along the Apennine foothills and on some Apennine outer fronts (Figure 2). Conversely, the seismicity is more sporadic in time and space north of the Po River. No significant historical or instrumental earthquakes are documented west of Milan, except for a few events in the Monferrato area.

Since also moderate earthquakes can produce extensive damage due to the high exposure of buildings and facilities, the identification and characterisation of poten-

tial seismogenic sources is crucial for mitigating the seismic risk. To locate the areas undergoing tectonic vertical deformation we adopted a geomorphological approach based on the analysis of the pattern and behaviour of the fluvial network. Alluvial rivers are very sensitive to modest ground tilting, to which they react with deflections and changes of their sedimentation pattern. We believe this approach is especially promising in areas such as the Po Plain, where the evolution of the drainage pattern is not affected by morphological obstacles nor controlled by bedrock heterogeneities. Only two anticlines are associated with a morphological expression (Figure 1): the Trino Vercellese Anticline (western Po Plain), which has about 40 m of relief and forces the Po River to follow an anomalous (anomaly #1 in Table 1); and the San Colombano Anticline (central Po Plain), associated with the sharp eastward deflection of the Lambro meridionale R. (anomaly #5 in Table 1). We used basic topographic data (topographic maps and DEM) to identify anomalous reaches along several alluvial rivers draining the Po Plain.

In general, anomalies in the drainage pattern may be ascribed to three main families of causes: climate, human activity and tectonic activity. Climate changes may induce rivers to cross critical erosional or depositional threshold values controlling major channel pattern changes (Schumm and Khan, 1972). Human activities may induce changes in the fluvial system by direct modifications of the channel (e.g.: engineering works and drainage regulation), by indirect alteration of the stream discharge and sediment load transport (Knighton, 1984), or by modifying the stream gradient through ground-water withdrawal. Tectonic activity produces longitudinal and lateral changes of the stream gradient, that alone may induce channel pattern shifts and diversions. These tectonic modifications, however, may accumulate and become apparent only in conjunction with extreme climatic events altering water discharge and sediment supply.

The anomalies we identified consist in river diversions, shifts in channel pattern and longitudinal changes of the channel behaviour. Due to their size, they are suggestive of the presence of active buried tectonic structures. Their true origin was assessed by spatial comparison between their location and the pattern of buried anticlines reported in the geological maps, and with the historical earthquakes listed in current catalogues.

We constructed a database of 36 anomalous reaches along more than 20 rivers. Each anomaly is believed to be evidence of the activity of a blind thrust (Table I). We could discriminate the seismic vs aseismic behaviour of the underlying fault only for a few cases where the anomaly is unambiguously associated with historical or instrumental seismicity.

We present as a case history the application of this approach to the identification of the source of the 12 May 1802 earthquake ($M_e$ 5.7), that struck the Oglio River Valley near Soncino (Cremona).

## 4.2. Geologic and geomorphic overview of the western Po Plain

### *4.2.1. Tectonic setting*

The geologic evolution of the Po Plain reflects the regional convergence between the African and European plates. This sedimentary basin is located at the northern termination of the Adria microplate, a promontory of the African plate. Since Late Cretaceous it represented the foreland of two chains of opposite vergence generated by the collision between the African and European plates (e.g.: Robertson and Grasso, 1995): the north-verging Apennines and the south-verging Southern Alps. Thrusting of these two chains loaded and flexed the Adria continental crust, giving rise to foredeep basins where a thick syn-orogenic clastic sequence was deposited (Doglioni, 1993, and references therein). As suggested by plate motion reconstructions (DeMets et al., 1994), and confirmed by seismicity (CPTI Working Group, 1999) relative motion between the two plates is ongoing with a convergence in a NNW-SSE direction, that geodesy indicate to have a rate of less than 1 cm/y (Ward, 1994; Anzidei et al., 2001). Part of this deformation is accommodated seismically within the thrust fronts of the two chains.

Due to the fast subsidence rates induced in the whole Po Plain area by the tectonic loading of the two chains, the more external fronts of the two thrust belts are buried beneath the plain. Therefore the main tectonic elements were mapped by means of the extensive seismic reflection data used for oil exploration (Pieri and Groppi, 1981). The map of the base of the Plio-Quaternary sequence south of the Po River (Pieri and Groppi, 1981) shows the occurrence of three arcs of blind, north-verging thrusts and folds that define the Apennine thrust fronts (from west to east, Figure 1): a) the Monferrato Arc (Elter and Pertusati, 1973); b) The Emilia Arc; and c) the Ferrara-Romagna Arc. The latter is further subdivided into three relatively minor structures: the Ferrara folds, the Romagna folds and the Adriatic folds. The Ferrara Folds ("Dorsale Ferrarese") are the most external structures of this arc. North of the Po River, the outer fronts of the Southern Alps thrust belt are arranged in a more simple pattern and deform the south-sloping Pedealpine homocline (Figure 1). The E-W continuity of the thrust front is interrupted by the Schio-Vicenza Line, an important transfer structure that separates the Po Plain thrust fronts to the west, from those of the Veneto Plain, to the east. In spite of the diffuse folding and thrusting imaged in the subsurface of the Po Plain by the geophysical exploration, very few tectonic structures are expressed at the surface. The most noticeable exceptions are represented by the Trino Vercellese Anticline, the San Colombano Anticline and the Montello Anticline in the Veneto Plain (from west to east, Figure 1). The Quaternary activity of these structures is testified by their influence on the drainage pattern and by the presence of young terraced surfaces tilted and uplifted along their flanks (Ferrarese et al., 1998; Benedetti et al., 2000; Castiglioni and Pellegrini, 2001).

During the Tertiary and the Quaternary, a considerable thickness of sediments was deposited in the Po Valley basin, on top of a sequence of Mesozoic passive margin carbonatic rocks. As a whole this clastic sequence is a regressive succession. Sediment sources included the Southern Alps and Apennines fold and thrust belts. On the southern side of the Po Plain, the Plio-Quaternary sediments in the foredeep

are 7-8.5 km thick (Doglioni, 1993). Sediments in the Southern Alps foredeep, are between 2 and 6 km thick (Doglioni, 1993; Bertotti et al., 1998).

### *4.2.2. Seismicity*

Most of the earthquakes listed in current historical catalogues are concentrated south of the Po River along portions of the pede-Apennines thrust front and on some buried Apennines outer fronts. Earthquakes are more infrequent north of the Po River and west of Milan, where only background micro-seismicity is recorded (Figure 2).

The most recent large earthquakes of the region occurred in 1971 and 1983 near Parma ($M_s$ 5.7 and 5.0, respectively), and in 1996 near Reggio Emilia ($M_s$ 5.1). The focal mechanism of the 1971 Parma event shows a reverse solution with a large strike-slip component (Anderson and Jackson, 1987). The Centroid Moment Tensor solutions of the 1983 Parma and 1996 Reggio Emilia events (CMT Harvard Catalogue, Dziewonski et al., 1983) show a thrust solution with a small strike-slip component, and with P-axis oriented N36°W and N24°W, respectively. This compressional tectonic regime is confirmed by the analysis of the Reggio Emilia main shock and related aftershocks (Selvaggi et al., 2001). The focal mechanisms are consistent with a N-S sub-horizontal $\sigma_1$. Similar results were reached by Frepoli and Amato (1997), who obtained N-S oriented compressional P-axes using fault plane solutions, and Montone and Mariucci (1999) with an analysis of borehole breakouts, that show $S_{Hmax}$ oriented perpendicular to the trend of the thrust fronts. Other recent instrumental earthquakes include the 2000 Reggio Emilia event ($M_w$ 4.5), the 2000 Faenza-Forlí sequence ($M_w$ 3.4-4.4), and the 2000 Monferrato event ($M_w$ 4.6).

### *4.2.3. Geomorphology*

The Po Plain stretches E-W across northern Italy for more than 40,000 km$^2$, and is the widest alluvial basin of the peninsula. It is delimited both south and north by the topographic highs of the Apennines and of the Alps, respectively, and to the east by the Adriatic coastline. The plain is locally up to 100 km wide, and is drained axially by the 652 km-long Po River. For most of its course the Po is an alluvial river characterised by a single meandering channel. Its catchment basin is larger than 70,000 km$^2$.

The Po Plain can be separated into several Quaternary geomorphological units (M.U.R.S.T., 1997; Marchetti, 2002, and references therein). The area located between the southern boundary of the Alps and the Po River is characterised by the presence of a wide low-gradient, south-sloping depositional surface of fluvio-glacial and fluvial origin. This outwash plain, locally named "Plain main level" ("*Livello fondamentale della pianura*" in Petrucci and Tavaglini, 1969), was built up during the last glaciation, when rivers flowing from the Alps were characterised by water discharge and sediment supply substantially larger than today (Marchetti, 1990, 1996). Abandoned paleo-channels seen on top of this surface are oversized with respect to the present hydrography, implying a change in discharge occurred at the end of the last glaciation which led to the erosion of the alluvial plain (Marchetti, 1996). The present drainage network flows in valleys deeply incised into the aggradation surface. Small

patches of early to middle Pleistocene fluvio-glacial deposits ("old terrace unit", Marchetti 2002), and moraine deposits of Pleistocene-Holocene age, near the outlets of the main Alpine valleys, border the Po Plain at the Alps foothills. South of the Po River the drainage network flows on top of a Holocene aggradation surface , which merges with the active alluvial plain of the axial Po River. Continuous sedimentation is suggested by buried archaeological artefacts ranging in age from the Neolithic period to the Middle Ages (Marchetti, 2002). Close to the Apennine margin this surface is covered by coalesced alluvial fans of the same age as the "Plain main level", overlain by older fans deposited during previous glacial maximums (Marchetti, 2002 and reference therein). In contrast with the rivers flowing from the Alps, the Po River and its right tributaries flow on top of an active alluvial plain.

## 4.3. Geomorphic indicators of growing anticlines

Growing anticlines and tilting over a wide region encompassing an anticline-syncline pair are the surface expressions of slip on an underlying buried thrust or reverse fault (e.g.: Yeats, 1986; Stein and Yeats, 1989) (Figure 3). There are numerous geological, geomorphic and landscape features that are sensitive to slip on a buried thrust fault: topography, the thickness and shape of growth strata, the erosional/depositional behaviour of the drainage network, and the geometry of any erosional and/or depositional surfaces. The drainage network is especially sensitive to vertical deformation and thus very useful for analysing low-relief areas, where few or no landforms constrain the location of active faults (Holbrook and Schumm, 1999; Schumm et al., 2000). Field studies and numerical models show that the interaction between drainage systems and tectonic sources is governed mainly by the geometry and kinematics of the tectonic source (e.g.: Champel et al., 2002) and by the relative size of the rivers (e.g.: Guccione et al., 2002). Fault characteristics control the pattern and style of surface deformation, whereas the capacity of the rivers to keep pace with the uplift relies on their size (see for example the longitudinal stream profiles in Burnett and Schumm, 1983).

The fault-induced permanent deformation of the Earth surface controls the drainage pattern and the associated geomorphic/sedimentary processes. In particular the uplifted area is subjected to erosion, lack of drainage and antecedence phenomena, while the subsiding area is subjected to attraction of drainage and deposition (Figure 3b). River diversions are the most clear indicators that the stream is approaching a rising anticline or entering a syncline. The evolution of sedimentation and topography and of the geometry of geomorphic features is controlled by the growth of the anticline and of the syncline, which may or may not have a perceptible morphologic expression depending on the ratio between tectonic and sedimentation rates. More specifically, if the rate of vertical tectonic displacement is higher than the sedimentation rate, the anticline will have a morphological expression and will be subjected to erosion, while the syncline will be represented by a depressed area that may be filled up with sediments. The evolution of the tectonic topography created by the growth

and lateral propagation of the anticline is controlled by linear and areal surface processes that tend to create a smoothed steady-state morphology (Champel et al., 2002).

When a river enters a zone of active subsidence or uplift it may change its graded longitudinal profile. The river may then cross the zone undergoing deformation, or be deflected by it (Holbrook and Schumm, 1999). The river incises the area of steepened gradients over the growing structure and aggrades where the slope again decreases downstream. Similarly, the increase or decrease in slope caused by an impeding zone of uplift or subsidence may alter the channel pattern of a river (braided, meandering or anastomosing) and its stream power. Variations of the stream power have a direct effect on the grain size of the stream bedload. In general, tectonically increased slopes will be characterised by increased bedload grain size, and viceversa (Ouchi, 1985). Deflection of the river around an area undergoing uplift or subsidence will appear as an abrupt shift in the river course coincident with the deformed zone (Holbrook and Schumm, 1999).

In addition to the deformation seen in a longitudinal profile, tectonic activity may also produce lateral shifting of a river (normal to the topographic gradient of the floodplain). Shifting may occur by sudden avulsion or slow migration (combing) of a stream toward the lower down-tilt part of the floodplain depending on the rate of lateral tilt (Peakall et al., 2000).

Schumm and Khan (1972) performed a series of experiments in a large flume to determine the effect of changing slope and sediment load on channel patterns. These experiments suggest that sediment loads and slopes are closely related, and that landforms may not always respond progressively to altered conditions. Rather, dramatic morphologic changes may occur abruptly when critical erosional and (or) depositional threshold values are exceeded.

All of the above effects may be recorded in the alluvial stratigraphic sequence, and their detailed study allows areas of persistent anomalies to be located and characterised. Unfortunately, such anomalies may arise also from non-tectonic processes that induce variations of the topographic gradient. For this reason, ruling out other explanations for the observed anomalies is important before they can be confidently interpreted as indicators of tectonic activity (Holbrook and Schumm, 1999).

## 4. The case of the Po Plain: river anomalies vs. subsurface data and seismicity

Very few anticlines in the Po Plain have a surface expression, probably because sedimentary rates outpace tectonic rates. For example, Vittori and Ventura (1995) proposed Late Pleistocene-Holocene sedimentation rates of 0.6. 2.1 mm/y for the central part of the basin. These estimates compare with preliminary slip and vertical displacement rates of 1.7 and 0.6 mm/y, respectively for the fault driving the Mirandola anticline, one of the fastest growing structures of the entire Po Plain (Ciucci et al., 2002; shown as n. 4 in Figure 1a). The *Geomorphological Map of the Po Plain* (M.U.R.S.T., 1997) shows numerous examples of drainage diversion which in some cases have been dated by radiometric and archaeological methods. This geomor-

phological record extends back in time to the beginning of the Holocene at the earliest, when morphogenic processes triggered by the last glacial maximum formed the "Plain main level" on the northern side of the Po Plain and started continuous fluvial aggradation on its southern side (Marchetti, 2002). In this context several rivers show an evolution of their pattern that is not random, but rather seems to be driven by long-lasting vertical motions that resemble the surface effects induced by the activity of blind thrusts. A striking example is given by the Po River just south of Mantova, whose course has been shifted northward possibly due to the activity of the Ferrara Folds, as suggested by the abandoned paleochannels south of its present position.

We analysed systematically the response of drainage to the tilt induced by folding. The drainage response varies in trend and strength depending on the location of each given stream section relative to the fault. To reproduce the indications arising from the geomorphological analysis, which constrain the location of the anticline/syncline couple, we use elastic dislocation modelling. Our approach assumes permanent deformation of an essentially unfractured uppermost portion of the crust, such that the direction and magnitude of tilting can be derived from the fault parameters via elastic dislocation theory. Our starting assumption is that where folds are not expressed at the surface and a thick alluvial bed isolates the drainage network from the fold, rivers should generally flow in the direction of the maximum topographic gradient. Regional topography of the Po Plain is indicated by contour lines that open eastward toward the Adriatic coastline, and by a central trough occupied by the Po River (see the colour coded topography in Figure 2). This pattern is the compounded result of regional uplift of the Northern Apennines (along a NW-SE axis) and Southern Alps (along a roughly E-W axis), infilling of the basin and subsequent eastward regression of the coastline. Local modifications of the regional slope are highlighted by drainage anomalies of the same wavelength: drainage in subsiding areas is marked by low slope and aggradation, whereas in uplifting zones by increased gradient and incision.

We adopted a quantitative method to locate areas undergoing local differential vertical motions, based on the detailed analysis of the topography and of the drainage network. To perform this analysis we used official topographic maps (IGMI, scale of 1:25.000), the regional *Map of Relief and Vertical Movements of the Po Plain* (scale 1:250,000) (M.U.R.S.T., 1997), and digital elevation models with the resolution of 230 m.

The methodology used to determine the presence of an anomaly in the flowing direction of the drainage network is shown in Figure 4. It consists in determining the average contour strike of the surface of the Plain main level (the depositional surface before the last deglaciation), with tangential segments along each contour line. The tangentials were taken at the down-slope convexities of the contour lines to reproduce with a maximum accuracy the pre-erosional surface. Maximum topographic gradient (red vectors in Figure 4) represents the direction orthogonal to these tangential lines, and we assume that drainage should flow in this direction. We then compared the flow direction of each river between the contour lines (dashed blue vectors in Figure 4), with the topographic gradients. We conventionally declared a drainage anomaly any time we found a divergence ≥10° between these two vectors. We also

considered the length of the reach over which the divergence persisted, adjusted to the river size. This is important to avoid sampling natural irregularities (such as large meanders) as anomalous reaches, and also because we expect that the size of the tectonically driven anomalies is related to the size of the underlying hidden fault. We declared an anomalous reach only if the divergence between the two vectors persisted for more than 5 km. This minimum length was chosen considering the average length of the longer meanders measured in the area. Besides being more easily detectable, larger anomalies imply bigger faults that may pose the largest hazard. For some rivers along which we identified such diversions, we searched for channel pattern shifts, using topographic maps and air photos interpretation.

We then removed all anomalies possibly correlated with human activity (artificial deviations, significant fluid withdrawal, etc.) or for which a tectonic origin can be easily ruled out, using ancient topographic maps and historical accounts. The remaining anomalies are listed in Table I, that summarises their main features and possible association with historical earthquakes.

Geological maps (1:100.000 scale) were used to compare spatially the anomalies with the position of structural axes, buried faults and lithological contacts. This step allowed us to correlate anomalies with buried tectonic structures. A further spatial comparison was made with the historical earthquakes listed in the *Catalogo Parametrico dei Terremoti Italiani* (CPTI Working Group, 1999). This second step suggested that the activity of at least some of the structures is potentially seismogenic. The observation of seismicity associated with a given anomaly supports the hypothesis of its tectonic origin.

Some of the areas where the above correlations appear to be most meaningful are shown in Figure 5. Areas outlined by black dotted circles exhibit strong correlation between drainage anomalies and buried anticlines (indicated with A and B, respectively). Areas indicated with A also exhibit some correspondence with historical seismicity. Areas shown as red dotted circles do not show any clear correlation and hence require further investigations. This is the case of Mantova (Mincio River, anomaly # 16), where a clear topographic and drainage anomaly is not related to any known structural element nor to historical earthquakes. In the area between the Secchia and Panaro rivers, the anomalies (# 24 and #26, Figure 5) are positively related with known large subsurface structures but there is no report of significant earthquakes. In the case of Verona (Adige River) the observed anomaly, can not be correlated to any known buried anticline, although it may be associated to slip on the fault responsible of the large 1117 earthquake ($M_e$ 6.6; CPTI Working Group, 1999).

## 4.5. A case history: anomalies of the Oglio River and the 1802 earthquake

The anomaly under examination (# 14, Table I and Figure 5) is represented by an abrupt southeastward turn of the Oglio River south of Soncino and Orzinuovi, towns located 35 km to NW of Cremona (Figures 4 and 5). A paleochannel located south of

the anomaly suggests a structural control on the river evolution (Figure 4). This section of the Oglio River exhibits anomalies both in terms of trend (SW diversion) and overall behaviour (increase of erosion power and sinuosity). These observations may all be explained with the presence of an area undergoing relative uplift affecting the river bed, and located south of the diversion.

To explore the longitudinal behaviour of the Oglio River we used a set of three different types of profiles (Figure 6): a longitudinal profile of the river bed, a topographic profile of the river banks, and a differential profile (difference between the previous two profiles). The differential profile was calculated to highlight the possible existence of reaches along which the river is actively eroding its bed, as a consequence of localised uplift. The first two profiles show that the river flows in a valley incised into the Plain main level by about 10 m (Figure 6a), whereas the third profile highlights that the differential relief reaches a maximum in the distance range 30-55 km, where relative uplift is inferred to be greatest. Most of the valley incision occurred at the end of the last glaciation, and it was the result of changes of water discharge and sediment supply. The two reaches up-stream and down-stream of the diversion are characterised by rather different longitudinal gradients, the higher being along the first reach. Instead, the topographic profile along the stream banks shows that there is a change in slope at about down-stream distance 20 km, that may correlate with the toe of the alluvial fan of the Oglio River. Up-stream of this point the profile is parallel to that of the river bed, indicating uniform erosion along this reach. We interpret the increase of the trend of the differential profile between distance range 30-55 km, as the result of localised uplift due to the growth of a buried anticline (Figure 6c). An additional indication comes from the longitudinal sinuosity profile (Figure 6b), which shows an increment at the beginning of the section characterised by the increase of relief, indicated by the presence of two peaks of high sinuosity. Sinuosity was calculated as the ratio between the true ($d_t$) and straightened ($d_s$) distance covered by the river along a given stretch, averaged over a distance of about 1 km:

$$\text{Sinuosity Index} = d_t / d_s$$

We interpret the two peaks of high sinuosity as a shortening of the wavelength of the meanders due to an obstacle to their down-stream migration.

A strong earthquake ($M_e$ 5.7) occurred on 12 May 1802 in the Oglio Valley, the flat area between Brescia and Cremona near Soncino (Figure 7). Over twenty towns were severely damaged, including Soncino, Crema, Brescia and Cremona, and among those Orzinuovi was the most seriously hit.

A solution obtained through the automatic elaboration of macroseismic intensity data using the Boxer code (Gasperini et al., 1999) yielded a hypothetical seismic source (Figure 7). This solution is in good agreement with indications supplied by subsurface geology, particularly as far as the orientation of the seismogenic structure is concerned. E-W buried anticlines belonging to the Alpine domain are commonly reported just south of a major drainage anomaly of the Oglio River (#14 in Table I

and Figure 5), which starts near Soncino and continues southward for approximately 25 Km. A geological section obtained from geophysical data (Cassano et al., 1986; inset in upper left corner of Figure 7) clearly shows the south-verging Alpine fronts which, near Cremona, face the north-verging thrusts of the Apennines domain.

Assuming that the above geomorphological observations can be explained by the activity of the causative fault of the 1802 earthquake, we calculated the expected displacement for unitary slip on a south-verging, 30˚-north dipping, blind thrust fault, extending from 3 to 6 km of depth (Table II). The vertical displacement that is expected to be generated by slip on such fault is shown in Figure 6c.

The size of the modelled fault is upper bounded by the magnitude of the 1802 earthquake, while its exact position is constrained by geomorphological observations along the Oglio River. We changed progressively the position of the modelled fault until the maximum of relative uplift (anticlinal axis) coincided with the maximum of the differential profile, and could explain the trend of the river itself and the presence of a paleochannel south of the divergence. Fault strike was constrained based on the average strike of the buried structures reported in the literature. The contours of the expected displacement of the fault model show an anticlinal uplift south of the diversion, and only slight subsidence north of it (Figure 8). Simple scaling relationships suggest that coseismic slip in 1802 was less than 0.5 m, yielding maximum surface vertical displacements of about 0.15 m.

Our understanding is that, after running into an anticline which slows down its natural course, the Oglio River was forced to leave the paleochannel and turn to the ESE. This diversion presumably occurred before the incision of the Plain main level started, because the reach down-stream the diversion is incised and the trace of the abandoned paleo-channel is on top of this surface. The extent of the diversion represents a balance between the stream power and the uplift rate of the anticline. The seismogenic sources inferred from macroseismic intensity data and geomorphic data do not completely overlap. The macroseismic source may have been influenced by the overestimation of intensity due to the structural weakness of buildings near Soncino at the time of the earthquake, as reported in "Catalogue of Strong Italian Earthquakes, 461 b. C. to 1997" (Boschi et al., 2000), or by an incomplete distribution of the dataset.

## 4.6. Discussion and conclusions

The morphological analysis carried out in this work revealed the occurrence of several anomalies of the drainage network in the Po Plain consisting mainly in river diversions. Changes in the channel pattern were highlighted in the few areas studied in better detail. To investigate their origin we compared their position and extent with the location of buried anticlines seen in commercial seismic sections or reported in geological maps.

We suggest that the anomalies included in our database represent the surface evidence of growing anticlines driven by blind thrusts. However, only occasionally

these anticline do have a discernible morphological expression, probably due to the competition between tectonic rates of vertical displacement and sedimentary rates. We suggest that slip on the blind thrust faults induces slight tilting of the surface that is enough to cause the deflection of the river network, even though it does not produce morphological anticlines.

We included in our database 36 drainage anomalies (Figure 5 and Table I), most of which occur in the southern part of the plain along tributaries of the Po River flowing down from the Apennines. All the anomalies except for four (#1, #2, #3, and #4) occur in the stretch of the plain east of Milan. The activity of the buried thrust fronts seems to have controlled also the Po River (#1, #32, #27 and #19), which exhibits shifts in channel pattern (e.g.: anomaly #32) and sudden diversions with abandoned paleo-channels (e.g.: anomaly #27).

The correlation of historical seismicity with some of these faults suggests that at least in some cases they slip seismically. The simple consideration that even in the most active areas of peninsular Italy the average return time for large earthquakes is longer than 1,000 years (e.g.: Figure 1 in Valensise and Pantosti, 2001a) suggests that current historical catalogues, which are considered complete for earthquakes larger than M 5.5 only after the XVII century A.D., may not cover a full seismic cycle for most of the seismogenic sources of the Po Plain, which could well be the site of very infrequent damaging earthquakes. A comparison between long-term (upper Pleistocene) and short-term vertical deformation rates, calculated using geomorphic correlations and repeated geodetic measurements respectively (De Martini et al., 1998), indicates that a large fraction of the strain is released aseismically for some of these active thrusts. If extended regionally, this observation would greatly reduce the seismic hazard of the Po Plain. This inference is supported by the difference between the large number of drainage anomalies that may be explained by the activity of blind thrusts, and the few large earthquakes listed in current catalogues.

We applied in detail a morphological analysis to the drainage anomaly shown by the Oglio River near Soncino (CR) (anomaly #14). Here we found a potential correlation among a river diversion, the longitudinal anomalies of the river bed (Figure 6), the presence of a buried anticline, and the occurrence of a $M_e$ 5.7 earthquake in historical times (Figure 7). Using simple dislocation model we speculate on the position and extent of the area undergoing differential vertical displacements. According to our hypothesis the geomorphic signal can be explained by the coseismic growth of an anticline located south of the diversion, driven by a south-verging, north-dipping blind thrust (Figure 8) belonging to the Southern Alps system. This fault model (Orzinuovi Source) has been included in the *Database of Potential Sources for Earthquakes larger than M 5.5 in Italy* (Valensise and Pantosti, 2001b) as a contribution for the seismic hazard assessment of the Po Plain. Four additional sources identified using the same method exist in the area (Figure 1), but only one of them was correlated to an historical earthquake (Bagnacavallo Source, # 5 in Figure 1 and Table II, associated with Anomaly #20-21 and 11 April 1688 earthquake in Table I).

## 4.7. References

Albarello, D., V. Bosi, F. Bramerini, A. Lucantoni, G. Naso, L. Peruzza, A. Rebez, F. Sabetta and D. Slejko (2000). Carte di pericolosità sismica del territorio nazionale, *Quaderni di Geofisica*, **12**.

Anderson, H. J. and J. A. Jackson (1987). Active tectonics of the Adriatic region, *Geophys. J. Royal Astonomical Society*, **91**, 937-983.

Anzidei, M., P. Baldi, G. Casula, A. Galvani, E. Mantovani, A. Pesci, F. Riguzzi and E. Serpelloni (2001). Insights into present-day crustal motion in the central Mediterranean area from GPS surveys, *Geophys. J. Int.*, **146**, (1), 98-110.

Bigi, G., A. Castellarin, R. Catalano, M. Coli, D. Cosentino, G. V. Dal Piaz, F. Lentini, M. Parotto, E. Patacca, A. Praturlon, F. Salvini, R. Sartori, P. Scandone and G. B. Vai (1989). Synthetic Structural-Kinematic Map of Italy, *C.N.R.-Progetto Finalizzato Geodinamica*. Reprinted in: G. B. Vai and I. P. Martini (eds), Anatomy of an orogen. the Apennines and adjacent Mediterranean basins. Kluwer Academic Publishers, Dordrecht, 495-512, 2001.

Benedetti, L., P. Tapponier, G. C. P. King, B. Meyer and I. Manighetti (2000). Growth folding and active thrusting in the Montello region, Veneto, northern Italy, *J. Geophys. Res.*, **105** (B1), 739-766.

Bertotti, G., V. Picotti and S. Cloetingh (1998). Lithospheric weakening during "retroforeland" basin formation. Tectonic evolution of the central South Alpine foredeep, *Tectonics*, **17** (1), 131-142.

Boccaletti, M., M. Coli, C. Eva, G. Ferrari, G. Giglia, A. Lazzarotto, F. Merlanti, R. Nicolich, G. Papani and D. Postpischl (1985). Considerations on the seismotectonics of the Northern Apennines, *Tectonophysics*, **117**, 7-38.

Boschi, E., E. Guidoboni, G. Ferrari, D. Mariotti, G. Valensise and P. Gasperini (2000). Catalogue of Strong Italian Earthquakes, 461 b. C. to 1997, *Annali di Geofisica*, **43** (4), 609-868.

Bullard, T. and W. Lettis (1993). Quaternary fold deformation associated with blind thrust faulting, Los Angeles Basin, California, *J. Geophys. Res.*, **98**, 8349-8369.

Burnett, A. W. and S. A. Schumm (1983). Alluvial-river response to neotectonic deformation in Louisiana and Mississipi, *Science*, **222**, 49-50.

Cassano, E., A. Anelli, R. Fichera and V. Cappelli (1986). Pianura Padana: interpretazione integrata di dati geologici e geofisici, 73∞ Meeting Società Geologica Italiana., September 29-October 4 1986, Rome, Italy, pp. 27.

Castiglioni, G. B. and G. B.Pellegrini (eds), (2001). Note illustrative della Carta Geomorfologica della Pianura Padana, Geografia Fisica e Dinamica Quaternaria, Suppl. **IV**, 207 pp.

Champel, B., P. Van Der Beek, J. L. Mugnier and P. Leturmy (2002). Growth and lateral propagation of fault-related folds in the Siwaliks of western Nepal. rates, mechanisms, and geomorphic signature, *J. Geophys. Res.*, **107** (B 6), 10.1029/2001JB000578, 2002.

Ciucci, F., P. Burrato and G. Valensise (2002). Complex geomorphic response to blind thrust faulting along the northern margin of the Apennines near Mirandola (Po Plain), in *Proceedings of the ESC Annual Meeting*, Genova, Italy, September 2002.

CPTI Working Group (1999). Catalogo Parametrico dei Terremoti Italiani, ING-GNDT-SGA-SSN, Bologna, pp. 88; http://www.ingv.it/.

Demets, C., R. G. Gordon, D. F. Argus and S. Stein (1994). Effect of recent revisions to the geomagnetic reversal time scale on estimates of current plate motions, *Geophys. Res. Lett.*, **21** (20), 2191-2194.

De Martini, P. M., P. Burrato and G. Valensise (1998). Active tectonic structures in the Padana Plain. new discrimination strategy from a joint study of geomorphic and geodetic leveling data, in *Proceedings of the EGS Annual Meeting*, Nice, France, April 1998.

Dolan, J. F., K. Sieh, T. K. Rockwell, R. S. Yeats, J. Shaw, J. Suppe, G. J. Huftile and E. M. Gath (1995). Prospects for larger or more frequent earthquakes In the Los Angeles metropolitan region, *Science*, **267**, 199-205.

Doglioni, C. (1993). Some remarks of the origin of foredeeps, *Tectonophysics*, **228**, 1-20.

Dondi, L. and M. G. D'andrea (1986). La Pianura Padana e Veneta dall'Oligocene superiore al Pleistocene, *Giornale di Geologia*, ser. 3$^a$, **48** (1-2), 197-225.

Dziewonski, A. M., A. Friedman, D. Giardini and J. H. Woodhouse (1983). Global seismicity of 1982: centroid moment tensor solutions for 308 earhquakes, *Phys. Earth Planet. Inter.*, **33**, 76-90.

Elter, P. and P. Pertusati (1973). Considerazioni sul limite Alpi-Appennino e sulle relazioni con l'arco delle Alpi occidentali, *Mem. Soc. Geol. It.*, **12**, 359-375.

Ferrarese, F., U. Sauro And C. Tonello (1998). The Montello Plateau, karst evolution of an alpine neotectonic morphostructure, *Z. Geomorph. N. F.*, Suppl.-Bd. **109**, 41-62.

Frepoli, A. and A. Amato (1997). Contemporaneous extension and compression in the Northern Appennines from earthquake fault-plane solutions, *Geophys. J. Int.*, **129**, 368-388.

Gasperini, P., F. Bernardini, G. Valensise and E. Boschi (1999). Defining seismogenic sources from historical earthquakes felt reports, *Bull. Seism. Soc. Am.*, **89** (1), 94-110.

Guccione, M. J., K. Mueller, J. Champion, S. Shepherd, S. D. Carlson, B. Odhiambo and A. Tate (2002). Stream response to repeated coseismic folding, Tiptonville dome, New Madrid seismic zone, *Geomorphology*, **43**, 313-349.

Hauksson, E., L. M. Jones, T. L. Davis, L. K. Hutton, G. Brady, P. A. Reasenberg, A. J. Michael, R. F. Yerkes, P. Williams, G. Reagor, C. W. Stover, A. L. Bent, A. K. Shakal, C. G. Bufe, M. J. S. Johnston, and E. Cranswick, (1988). The 1987 Whittier Narrows earthquake in the Los Angeles metropolitan area, California, *Science*, **239**, 1409–1412.

Holbrook, J. and S. A. Schumm (1999). Geomorphic and sedimentary response of rivers to tectonic deformation: a brief review and critique of a tool for recognizing subtle epeirogenic deformation in modern and ancient settings, *Tectonophysics,* **305**, 287-306.

Knighton, D. (1984). Fluvial forms and processes, Edward Arnold (ed), 218 pp.

Lin, J. and R. Stein (1989). Coseismic folding, earthquake recurrence and the 1987 source mechanism at Whittier Narrows, Los Angeles basin, California, *J. Geophys. Res.*, **94**, 9614-9632.

Marchetti, M. (1990). Cambiamenti idrologici nella Pianura Padana centrale a nord del fiume Po: i casi di "underfit streams" dei fiumi Mincio, Oglio e Adda, *Geogr. Fis. Dinam. Quat.*, **13**, 53-62.

Marchetti, M. (1996). Variazioni idrodinamiche dei corsi d'acqua della Pianura Padana centrale connesse con la deglaciazione, *Il Quaternario*, **9** (2), 465-472.

Marchetti, M. (2002). Enviromental changes in the central Po Plain (northern Italy) due to fluvial modifications and anthropogenic activities, *Geomorphology*, **44**, 361-373.

Massonet, D., M. Rossi, C. Carmona, F. Adragna, G. Peltzer, K. Feigl and T. Rabaute (1993). The displacement field of the Landers earthquake mapped by radar interferometry, *Nature*, **364**, 138-142.

Montone, P. and M. T. Mariucci (1999). Active stress along the NE external margin of the Apennines: the Ferrara arc, northern Italy, *Geodynamics*, **28**, 251-265.

M.U.R.S.T. (1997). Geomorphological Map of Po Plain, 1:250000 scale, S.E.L.C.A., Firenze.

M.U.R.S.T. (1997). Map of relief and vertical movements of Po Plain, 1:250000 scale, S.E.L.C.A., Firenze.

Ouchi, S. (1985). Response of alluvial rivers to slow active tectonic movement, *Geol. Soc. Amer. Bull.*, **96**, 504-515.

Peakall, J., M. Leeder, J. Best and P. Ashworth (2000). River response to lateral ground tilting: a synthesis and some implications for the modelling of alluvial architecture in extensional basins, *Basin Research*, **12**, 413-424.

Petrucci, F. and S. Tagliavini (1969). Note illustrative della Carta Geologica d'Italia, Foglio 61, Cremona, Servizio Geologico d'Italia, pp. 43.

Pieri, M. and G. Groppi (1981). Subsurface geological structure of the Po Plain, C.N.R., *P. F. Geodinamica*, Pubbl. **414**, 278-286.

Robertson, A. H. F. and M. Grasso (1995). Overview of the late Tertiary-Recent tectonic and paleo-environmental development of the Mediterranean region, *Terra Nova*, **7**, 114-127.

Schumm, S. A., J. F. Dumont and J. M. Holbrook (2000). Active tectonics and alluvial rivers, *Cambridge University Press*.

Schumm, S. A. and H. R. Khan (1972). Experimental study of channel patterns, *Geol. Soc. Amer. Bull.*, **83**, 1755-1770.

Selvaggi, G., F. Ferulano, M. Di Bona, A. Frepoli, R. Azzara, A. Basili, C. Chiarabba, M. G. Ciaccio, F. Di Luccio, F. P. Lucente, L. Margheriti and C. Nostro (2001). The $M_W$ 5.4 Reggio Emilia 1996 earthquake: active compressional tectonics in the Po Plain, Italy, *Geophys. J. Int.*, **144**, 1-13.

Shaw, J. H. and J. Suppe (1996). Earthquake hazards of active blind-thrust faults under the central Los Angeles basin, California, *J. Geophys. Res.*, **101**, 8623-8642.

Stein, R. S. and R. S. Yeats, (1989). Hidden earthquakes, *Scientific American*, **260**, 48-57.

Suppe, J., G. T. Chou and S. C. Hook (1992). Rates of folding and faulting determined from growth strata, in: K. R. McClay (ed), Trust Tectonics. Chapman and Hall, New York, 105-121, 1992.

Valensise, G. and D. Pantosti (2001a). The investigation of potential earthquakes sources in peninsular Italy: A review, *J. of Seismology*, **5**, 287-306.

Valensise, G. and D. Pantosti (eds) (2001b). Database of Potential Sources for Earthquakes larger than M 5.5 in Italy, Annali di Geofisica, Suppl. to vol. **44** (4), 180 pp., with CD-ROM.

Vittori, E. and G. Ventura (1995). Grain size of fluvial deposits and Late Quaternary climate: a case study In the Po River valley (Italy), *Geology*, **23**, 735-738.

Ward, S. N. (1994). Constraints on the seismotectonics of the central Mediterranean from Very Long Baseline Interferometry, *Geophys. J. Int.*, **117**, 441-452.

Wright, T. L. (1991). Structural geology and tectonic evolution of the Los Angeles basin, California, In: Biddle, K. T. (Ed.), Active Margin Basin, *American Association of Petroleum Geologists Memoir*, **52**, 35-134.

Yeats, R. S. (1986). Active faults related to folding, In R. E. Wallace (ed), Active tectonics, National Academy Press, Washington, 63-79.

| Id | River name | Location of anomaly | Anomaly type | Length of anomalous reach (km) | Anomaly rating | Subsurface anticline | Topographic expression | Sheet # (1:100.000) | Associated historical earthquake(s) ($M_e$) | Distance from anomaly (km) |
|---|---|---|---|---|---|---|---|---|---|---|
| 1 | Po | Montarolo (VC) | CP/D | 36.0 | A | Y | Y | 57 | | |
| 2 | Sesia | Palestro (VC) | D | 22.4 | B | | | 57/58 | | |
| 3 | Agogna | Vespolate (NO) | D | 13.9 | C | Y | | 58 | | |
| 4 | Agogna | Ottobiano (PV) | CP | 7.6 | C | Y | | 58 | | |
| 5 | Lam- | S. Colombano (LO) | D/CP | 26.4 | A | Y | Y | 59/60 | | |
| 6 | Adda | Rivolta d'Adda (BG) | CP | 13.3 | B | Y | | 46 | | |
| 7 | Adda | Cornegliano/Cavia ga | CP/D | 48.7 | A | Y | Y | 60 | 1786 4 7 (5.2) | 0.0 |
| 8 | Brembiolo | Casalpusterlengo (LO) | D | 7.0 | C | Y | Y | 60 | | |
| 9 | Serio | Bariano (BG) | CP | 8.7 | C | | Y | 46 | | |
| 10 | Serio | Malpaga (BG) | CP | 8.2 | C | | | 46 | | |
| 11 | Oglio | Romano di Lombardia | CP/D | 15.3 | A | | | 46 | | |
| 12 | Mella | Poncareale (BS) | CP/D | 10.4 | B | Y | Y | 47 | | |
| 13 | Mella | Bassano Bresciano (BS) | CP/D | 13.0 | A | Y | | 47/61 | | |
| 14 | Oglio | Soncino (CR) | D/CP | 79.5 | A | Y | Y | 60/71 | 1802 5 12 (5.6) | 9.8 |
| 15 | Mincio | Goito (MN) | D | 8.9 | B | | | 62 | | |
| 16 | Mincio | Mantova (MN) | D | 23.8 | A | | Y | 62 | | |
| 17 | Adige | Verona (VR) | D/CP | 29.4 | A | | | 49 | 1117 1 3 (6.6) | 4.6 |
| 18 | Adige | Legnago (VR) | CP | 14.9 | C | | | 63 | | |
| 19 | Po | Ficarolo (RO) | D | 36.0 | B | Y | | 76 | | |
| 20 | Lamone | Alfonsine (RA) | D/CP | 14.9 | A | Y | | 89 | 1688 4 11 (5.7) | 8.7 |
| 21 | Senio | Cotignola (RA) | D/CP | 19.4 | A | Y | | 88 | 1688 4 11 (5.7) | 0.0 |
| 22 | Idice | Budrio (BO) | D | 26.4 | B | Y | | 88 | 1796 10 22 (5.7) | 6.5 |
| 23 | Reno | S. Agostino (BO) | D | 37.6 | A | Y | | 75 | | |
| 24 | Panàro | Bomporto (MO) | D/CP | 30.0 | A | Y | | 75 | | |
| 25 | Panàro | Castelfranco Emilia | CP | 32.6 | A | Y | | 87 | | |
| 26 | Secchia | Mirandola (MO) | D/CP | 43.8 | A | Y | | 75 | | |
| 27 | Po | Guastalla (RE) | D/CP | 28.6 | A | Y | | 74 | | |
| 28 | Crostolo | Reggio Emilia (RE) | D | 10.7 | C | Y | | 74/86 | 1438 6 11 (5.5)<br>1831 9 11 (5.3)<br>1832 3 13 (5.5)<br>1971 7 15 (5.6) | 6.0 - 20.0 |
| 29 | Enza | Monticelli Terme (PR) | CP/D | 17.3 | A | Y | | 73 | | |
| 30 | Parma | Parma (PR) | CP/D | 20.5 | A | Y | | 73 | | |
| 31 | Arda | Cortemaggiore (PC) | D | 13.8 | B | Y | | 72/73 | | |
| 32 | Po | Cremona (CR) | CP/D | 36.4 | A | Y | | 60 | | |
| 33 | Nure | S. Polo (PC) | CP | 8.7 | C | Y | | 60/72 | | |
| 34 | Nure | S. Giorgio Piacentino | CP | 5.0 | C | Y | Y | 72 | | |
| 35 | Trebbia | Maniaco (PC) | CP | 6.8 | C | Y | | 60 | | |
| 36 | Tidone | Pontetidone (PC) | CP | 10.0 | C | Y | | 60 | | |

**Table I.** List of the drainage anomalies identified in the Po Plain and positively related to a tectonic origin (ID numbers as in Figure 5). The main types of anomaly that were recognised are drainage diversions (D) and channel pattern shifts (CP). The rating of the anomalies is based on the length of the anomalous reach, on the type of anomaly. And in the case of diversions it is also based on the angle of diver-

gence between the mean flow direction and the direction of the maximum topographic gradient (see chapter 4 for details). Higher ratings (A) were assigned to anomalies characterised by longer anomalous reaches and diversions (D) associated with channel pattern shifts (CP). Historical earthquakes tentatively associated to each anomaly are shown along with minimum epicentral distance from the anomalous reach ($M_e$ from CPTI Catalogue, 1999). The last column lists how much we rely on the tectonic origin of the anomaly, based on all considerations. Anomalies # 28, 29 and 30 occur within 20 km of the epicentral location of the four historical earthquakes listed in the nearby cell.

| # | Source Name | Length Km | Width Km | Strike | Dip | Rake | Min Depth Km | Max Depth Km |
|---|---|---|---|---|---|---|---|---|
| 1 | Orzinuovi | 10.0 | 6.0 | 266° | 30° | 90° | 3.0 | 6.0 |
| 2 | Mantova | 10.0 | 6.0 | 262° | 30° | 90° | 3.0 | 6.0 |
| 3 | Adige Plain | 15.0 | 8.5 | 255° | 30° | 90° | 3.0 | 7.3 |
| 4 | Mirandola | 12.0 | 10.0 | 115° | 30° | 90° | 3.0 | 8.0 |
| 5 | Bagnacavallo | 10.0 | 6.0 | 119° | 30° | 90° | 3.0 | 6.0 |
| 6 | Asolo | 27.0 | 9.0 | 149° | 80° | 170° | 1.0 | 9.9 |
| 7 | Montello | 15.0 | 8.0 | 234° | 30° | 90° | 2.0 | 6.0 |
| 8 | Alpago | 18.0 | 9.0 | 206° | 55° | 50° | 1.0 | 8.4 |
| 9 | Cansiglio | 12.0 | 7.3 | 230° | 50° | 64° | 1.0 | 6.6 |
| 10 | Pordenone N. | 8.0 | 5.5 | 215° | 30° | 80° | 2.0 | 4.8 |

**Table II.** Parameters of the seismogenic sources of the Po and Veneto plains included in the *Database of Potential Sources for Earthquakes larger than M 5.5 in Italy* (Valensise and Pantosti, 2001b). Each source is keyed to Figure 1 through a code. The Orzinuovi seismogenic source (#1) is related to the 12 May 1802 Valle dell'Oglio earthquake, and was identified through the geomorphological approach presented in this work. Its geometrical and kinematic parameters were used for the dislocation modelling (see Figure 8).

**Figure 1.** (A) Simplified structural map of the Po Plain and neighboring Veneto Plain, showing the main tectonic elements (from Pieri and Groppi, 1975, modified), and contours of the base of the Plio-Quaternary sedimentary sequence (from Bigi et al., 1989). The plain is shaded in light grey, while higher topography regions are shown in white. The outer thrust fronts of the southern Alps and of the Apennines are buried beneath the thick syn-orogenic clastic deposits. The seismogenic sources are from Valensise and Pantosti (2001b) and are identified in Table II. (B) Structural cross-section of the central Po Plain, showing the main buried thrust fronts of the northern Apennines and southern Alps (from Cassano et al., 1986, modified). Location of the trace is shown in Figure 1a.

**Figure 2.** Historical seismicity of the Po Plain (CPTI Working Group, 1999). The focal mechanisms of the three largest instrumental earthquakes recorded in the area are

consistent with ongoing N-S contraction. In contrast, seismicity recorded in the inner portions of the Apennines chain is mainly extensional. Only a few earthquakes are reported north of the Po River, and seismicity does not follow a regular pattern.

**Figure 3.** Schematic representation in map view (above) and cross-section (below) of the effects that slip on a generic blind, low-angle thrust fault may have on geomorphic/sedimentary processes. The vertical component of the expected deformation is related to the fault's geometry and kinematics through the elastic dislocation theory. Evolution of sedimentation and drainage pattern over a wide area is controlled by the growth of the anticline/syncline, which produces tilting of the ground surface.

**Figure 4.** Outline of the method used to detect drainage anomalies in the Po Plain. The figure shows an area located north of the Po River, between the Adda River and the Mella River. Straight-line segments at contour line intervals ranging between 5 and 10 m were constructed from the Map of Relief and Vertical Movements of the Po Plain (M.U.R.S.T., 1997). (Solid red arrows and dashed blue arrows show topographic gradients and actual average drainage directions, respectively. We defined a drainage anomaly as a ≥10° divergence between the two vectors. Anomaly #14 on the Oglio River is analysed in detail. *A* and *B* mark the ends of profiles shown in Figure 7.

**Figure 5.** Distribution of drainage anomalies in the Po Plain (marked in yellow). Dashed black circles labelled A outline areas where an anomaly, a fold axis, and a historical earthquake coincide. Dashed black circles labelled B indicate areas where surface evidence corresponds to buried anticlines, but no historical earthquakes are reported. Dashed red circles highlight areas that require further investigations: see text for discussion. Drainage anomalies are numbered according to Table 1.

**Figure 6.** Profiles of the Oglio River from the Alpine frontal moraines to the confluence with the Mella River. **(a)** The differential profile, obtained by subtracting the elevation of the river bed from the average elevation of the Plain main level, shows a dramatic increase of incision in the distance range 30-50 km, suggesting that the river meets an area of localised uplift. **(b)** an increment of sinuosity highlighted at about 30 Km from the upper-end of the section is possibly related to a variation of the longitudinal slope of the river bed. **(c)** expected vertical displacement along the river bed generated by slip on a blind, 30°-north dipping thrust fault (full faulting parameters and location of the modelled fault shown in Figure 8 and Table II). This fault explains the geomorphic observations (longitudinal anomalies of the Oglio River as well as its SE-diversion) and fits subsurface geological data (see upper-left inset of Figure 6). We suggest that this fault is the causative source of the 1802 earthquake.

**Figure 7.** Intensity data for the 12 May 1802, $M_e$ 5.7 earthquake (Boschi et al., 2000), the Oglio River anomaly (#14), and buried anticlinal axes from geological maps.

Two fault models respectively obtained from intensity data (using the Boxer code, Gasperini et al., 1999) and geomorphological observations (this work) are shown for comparison. The black line is the trace of the geological section obtained from geophysical data shown in the upper left corner (from Cassano et al., 1986, modified). It shows that in this area the south-verging Alpine front faces the north-verging Apennine outermost fronts. We propose that the seismogenic source of the 1802 earthquake is a south-verging blind thrust fault belonging to the Alpine system.

**Figure 8.** Summary map showing the position of the proposed causative fault of the 12 May 1802 earthquake, contours of the expected vertical displacement and comparison with the geomorphic observations. Since this is a qualitative test of fault activity, all displacements are referred to unitary slip. Due to the lack of reliable strain and chronological markers, we did not attempt to estimate true cumulative slip and slip rate. The contours express the ratio between slip at depth and surface displacement (e.g., for 1 meter slip top uplift is 0.3 m). Positions of the buried anticlinal axes and the paleo-channel south of the river diversion are shown. The geometry and location of the modelled fault are constrained using both geomorphological and subsurface geology observations. The abandonment of the paleochannel and the longitudinal anomalies observed along the Oglio River are induced by fault-related tectonic uplift south of the diversion. Topography is from the Map of Relief and Vertical Movements of the Po Plain (M.U.R.S.T., 1997).